Comput. Math. Applic. Vol. 14, No. 9–12, pp. 699–739, 1987
Printed in Great Britain.

0097-4943/87 $3.00 + 0.00

INHERITED RATE MODEL OF THE CELL CYCLE: KINETICS OF RELATED CELLS, EPI-GENETICS OF RIBOSOMAL DNA TRANSCRIPTION AND THE EVALUATION OF CANCER-THERAPY FRACTIONATION SCHEDULES AND DOSES

D. R. RIGNEY†
Institute for Cancer Research, Fox Chase Cancer Center, 7701 Burholme Avenue, Philadelphia, PA 19111, U.S.A.

Abstract—A two-variable, stochastic model of the mammalian cell cycle is proposed for the interpretation of correlations between the intermitotic times of related cells, for the analysis of heterogeneous silver staining patterns that are seen at the nucleolar organizer regions (NORs) of chromosome spreads, for the analysis of fraction-labeled-mitoses curves and for simulating the outcome of chemotherapeutic protocols having different doses and fractionation schedules.

One of the model's variables represents the chromatin condensation/replication cycle. The second variable is related to the cell's ability to grow: the number of fibrillar centers in the cell's nucleoli, in excess of the minimum number found in quiescent cells. The number of these centers is assumed to increase and decrease at random, with transition rates that are functions of the growth conditions. The chromatin variable is postulated to increase at a rate proportional to the nucleolar variable (through a mechanism involving ubiquitin), so that the cell's generation time will also be random. The number of fibrillar centers in a mitotic mother cell persists in newly-formed daughter cells, providing a mechanism for positive correlation between sibling and mother–daughter cell generation times.

Expressions for the following quantities are provided as a function of the model's parameters: the average, variance and higher moments of the intermitotic time, the distribution of the number of fibrillar centers, the joint distribution of sibling, mother and daughter cell intermitotic times, the Malthusian parameter of exponential population growth, numbers that describe the damped oscillation of a perturbed population and the entropy of a cell population.

1. INTRODUCTION

> "The most formidable obstacle to the successful treatment of disseminated cancer may well be the fact that the cells of a tumor are biologically heterogeneous .... Cells isolated from one tumor have been shown to differ with respect to their growth rate, karyotypes, cell surface receptors for lectins, hormone receptors, immunogenicity, response to cytotoxic agents, and capacity for invasion and metastasis .... A tumor may contain as many as 10^9 cells; eradication of 99.9% of these cells still leaves 10^6 cells to proliferate, thus providing a large base for the further generation of biological heterogeneity" [1].

One of the primary goals of current cancer research is to understand the mechanisms responsible for the generation of phenotypic diversity in cell populations [1–6]. The aim of this paper is to present a quantitative model for two interrelated types of such cellular heterogeneity: (i) cell-to-cell variation in intermitotic times; and (ii) variation in the levels of synthesis of particular gene products. The model that is presented is called the inherited rate model [7]. It addresses four specific problems and several general issues.

The first problem is to understand in mechanistic terms why cells throughout even a genetically homogeneous population have heterogeneous intermitotic times, but that sibling cells and mother and daughter cells have intermitotic times that are more similar than randomly selected pairs of cells. The explanation proposed here is that cells are heterogeneous with regard to the activity of their nucleoli, that this heterogeneity of nucleolar activity provides a mechanism for the heterogeneity of intermitotic times and that the level of nucleolar activity is passed from one

†Present address: Cardiovascular Division, Harvard Medical School, Beth Israel Hospital, 330 Brookline Avenue, Boston, MA 02215, U.S.A.

generation to the next in an epi-genetic fashion, providing a mechanism for the correlation between the intermitotic times of related cells.

The second problem is the reverse of the first, to interpret cell-to-cell heterogeneity of nucleolar activity when information concerning the heterogeneity of intermitotic times is also available. The nucleolar activity may be shown to be heterogeneous by examining the amount of silver staining of the nucleolar organizer regions (NORs) among chromosome spreads.

The third problem is to estimate cell kinetic parameters from fraction-labeled-mitoses and related experimental procedures. There are circumstances in which data obtained by these methods are difficult to fit using currently available models, and the model described here may be useful in some such circumstances.

The fourth problem is that of designing radiation and chemotherapeutic protocols. The model may be used to simulate potential protocols, with the objective of evaluating alternate strategies. Applicability of the model is dependent on the cell-to-cell heterogeneity of response to cytotoxic agents being correlated with other types of cellular variability.

Before formulating a model for the analysis of these specific quantitative problems, it was necessary to consider the following general issues. What variables should be included in the model? What happens to the variables when a cell divides? What properties must the model exhibit in order that it be qualitatively correct?

Selection of variables to represent cell growth and division

The growth and division of cells are, in the final analysis, a set of chemical reactions involving the macromolecules that constitute the cell. A comprehensive model of a cell population would be one in which these reactions are represented explicitly [8–12], but it is not yet possible to implement such a model realistically: (i) a mammalian cell may contain some 10,000 messenger RNA species, most of which are present at less than 20 molecules/cell [13]; (ii) few of the proteins coded by these messengers have been characterized, and they are segregated into different organelles by an elaborate, dynamic membrane system [14–17]; and (iii) the large-scale configuration of the cell, organized by the cytoskeleton and nuclear matrix, is poorly understood [18–22]. This is not to say that a tractable model of the cell cycle cannot be correct, but rather that at the current state of the art, models should be designed with the following objective in mind—that they can be adapted or expanded to interpret the influence of a variety of particular variables on the kinetics of cell growth and division, without making explicit reference to the thousands of other variables that might have been investigated. The situation that arises in practice is that the cell-to-cell distribution of only one or a few variables will have been measured, and it is desired to use these data to predict the distribution that would be measured under other growth conditions. The distribution of DNA content, measured by flow cytometry, is the property that is most frequently analyzed [23, 24]. Another property that is commonly measured is cell size, and models are used to examine the question of whether growth beyond a certain size is required for cell cycle progress [25–28]. Total cell protein or RNA content have also been analyzed by similar methods [29]. It is likely that many related problems will arise in the future since an increasing number of hybridization, antibody and fluorescent probes are being used for the single-cell measurement of nucleic acids, proteins and other cell properties [30, 31]. There is already a literature on the possibility that cell-to-cell variability in the number of growth-factor receptors is responsible for the variability of intermitotic times [32, 33]. How do we model the kinetics of their participation in the growth and division cycle?

Heritability of cell properties

In contrast to the DNA content of diploid cells, the cell's content of other components is variable, because other components do not have mechanisms for exact duplication and equi-partition between daughter cells. Therefore, any model for the level of these other components must account for the variability that is due to inheritance, as well as the variability that would arise if all newly-formed cells were identical. The transmission of substances to daughter cells may be equal, random or asymmetric [34–36], and a model that describes the propagation of a substance over several generations must be specific about the way that the partitioning occurs.

Models for correlations between the intermitotic times of related cells

Cells in the same population have a dispersion of generation times, but the generation times of sibling and mother–daughter cell pairs are correlated [37]. Models that predict these correlations have been proposed as representations of mechanisms for the control of cell cycle events [28, 38, 39]. They attempt to explain the correlations either through the inheritance of some property or through the existence of a process that overlaps more than one generation. These models are consistent with the observation of a positive correlation between the generation times of sibling cells but are distinguishable on the basis of their predictions concerning the correlation between mother and daughter cells. Representative examples are the model proposed by Koch and Schaechter [40] and the "transition probability" model [41, 42]. For the reasons explained below, they are unsuitable for situations in which mother and daughter cell generation times are observed to be positively correlated.

The model of Koch and Schaechter [40] is based on the proposition that DNA replication begins when a cell reaches a "critical size" and that there are similarities between the initial sizes of sibling cells. Its prediction of a negative mother–daughter correlation may be understood from the following reasoning. If by chance a mother cell divides earlier than average, it will most likely be smaller than average. The daughter cells will therefore be smaller than average and have a generation time that is longer than average, by the amount that is required for growth to the average size of a newly-formed cell. The reverse is true when a mother cell divides with a size that is larger than average, so the mother–daughter correlation is negative. A model of this sort may be appropriate for bacteria and lower eukaryotes, in which negative mother–daughter correlations are observed [28].

The "transition probability" cell cycle model, on the other hand, allows no correlation between the generation times of mother and daughter cells. It postulates the existence of a process that begins at random during or after the S phase in a mother cell, that progresses in parallel with the chromosome replication/condensation cycle, and that continues to completion in the G1 phase of newly-formed daughter cells. Since the time that a cell spends in the S, G2 and M phases is treated as independent of the (random) fraction of the parallel process that is to be completed in its daughter cells, the model provides no mechanism through which mother and daughter intermitotic times can be correlated.

Mother and daughter cell generation times are observed to be positively correlated in eukaryotic cell populations [28, 43–48] so neither a "critical size" model nor an "overlapping parallel process" model can be a complete representation of the cell cycle, at least in their simplest forms. Reports that the mother–daughter correlation is nearly zero are rare [49], and even then the authors mention additional experiments in which the correlation was observed to be significantly greater than zero [42, p. 503]. The model that is developed here accounts for the positive correlation by assuming that cells inherit factors that influence the rate of cell cycle progression. It is therefore conceptually similar to rate models that do not predict the mother–daughter correlation [50, 51]. It is also similar to maturity models of the cell cycle [52–55], which emphasize the velocity of cell cycle maturation. However, it is different from other models in that it focuses on a single, heritable property that can be shown to be heterogeneous in individual, mitotic cells, namely, the activity of nucleoli.

2. BACKGROUND INFORMATION CONCERNING NUCLEOLI AND THE CELL CYCLE

The model to be described in the next section represents the state of a cell by two variables. The first variable denotes cell cycle maturity, and the second variable describes the state of a cell's nucleoli. The purpose of this section is to explain in experimental terms what these variables represent—they are not hypothetical concepts. Such concreteness is essential if the form of the model is to be believed and if it is to be expanded realistically to include additional variables, such as the cell's content of growth-factor receptors.

A. Meaning of the Term "Cell Cycle"

Many cell cycle models include a variable to represent the physiological maturity of a cell, but

their authors rarely commit themselves to a physical meaning for the variable. Rotenberg [54] posed the problem as follows:

> "There is the practical problem of determining [a cell's] physiological age; it is simple enough in S phase using DNA content, but so far adequate markers in G1 and G2M are not available. There is the further question of the dimensionality of [a cell's physiological maturity]. Simultaneous markers (DNA content, cell volume, [postulated] substances such as initiator protein, tubulin etc.) may follow one another, but others will proceed in parallel and will require that [the maturity variable] be a vector."

The difficulty in defining the cell cycle as a strictly biochemical series of events is that the activity of relatively few macromolecules change more than a modest amount as a function of cell age in actively proliferating populations [56–58]. Exceptions are those proteins that are clearly associated with the S phase itself (histones, thymidine kinase etc.). If we expand the definition of the cell cycle to include the events following the stimulation of hormonally, nutritionally or density inhibited cells (G0 → S) then the use of macromolecular markers to define cell cycle events is much more attractive. In that case, the induction of a series of growth-factor-related macromolecules may be demonstrated [59, 60]. Even so, the definition of cell cycle progress in terms of a particular series of mRNA or protein levels is problematic. The mitogenic role of these growth-factor-related events may be to bring about global changes in calcium levels, pH, general states of protein phosphorylation etc. that are the proximal cause of the G0 → S phase transition and might be bypassed or absent under some circumstances [61, 62].

An alternative to a strictly biochemical definition of cell cycle maturity has been available for several decades. Mazia [63] proposed that the events of mitosis, in which chromosomes achieve a highly condensed configuration, are part of a continuum of relaxation and condensation that occurs throughout the life of a cell: the chromosomes progressively relax during G1, achieve an extended configuration in the S phase, and—when the synthesis of chromatid pairs is complete—progressively recondense during G2 until the tight mitotic configuration is re-achieved. From this perspective, the cell cycle maturity of a cell may be determined by forcing its chromosomes to condense prematurely in order to see how tight they become, relative to the chromosomes in a mitotic cell [64–66]. Different degrees of condensability, corresponding to different levels of cell cycle maturity, are shown in Fig. 1. This definition of maturity may be used for G1, G2 and mitotic cells, but it is inadequate for S phase cells since they appear to be totally decondensed throughout that phase. The level of DNA content might be used to define the maturity of an S phase cell, but this is not ideal since chromosome duplication occurs in phases in diploid cells. Rather, the sequence of chromosome band replication is a more appropriate definition of S phase maturity [67–69] and may be demonstrated by bromodeoxyuridine pulse labeling methods, as shown in Fig. 2.

To summarize our definition of the cell cycle maturity for cells in an actively proliferating population: successive stages of G1 correspond to progressively relaxed single-chromatid chromosomes, the stages of the S phase correspond to a sequence of chromosome band replication, and successive stages of G2 and M correspond to progressively condensed double-chromatid chromosomes. It should be noted that the degree of chromosome condensation may be defined by procedures other than premature condensation and may lead to somewhat different operational definitions of cell cycle maturity [70–74].

B. Biology of Nucleoli

The second variable of the model describes objects found in a cell's nucleoli. The following paragraphs summarize the biology of nucleoli, with the aim of indicating what properties may be measured in individual cells, how they are passed from one generation to the next and how they are related to the rate at which a cell progresses through the cell cycle (the first variable, which is defined in the previous paragraph).

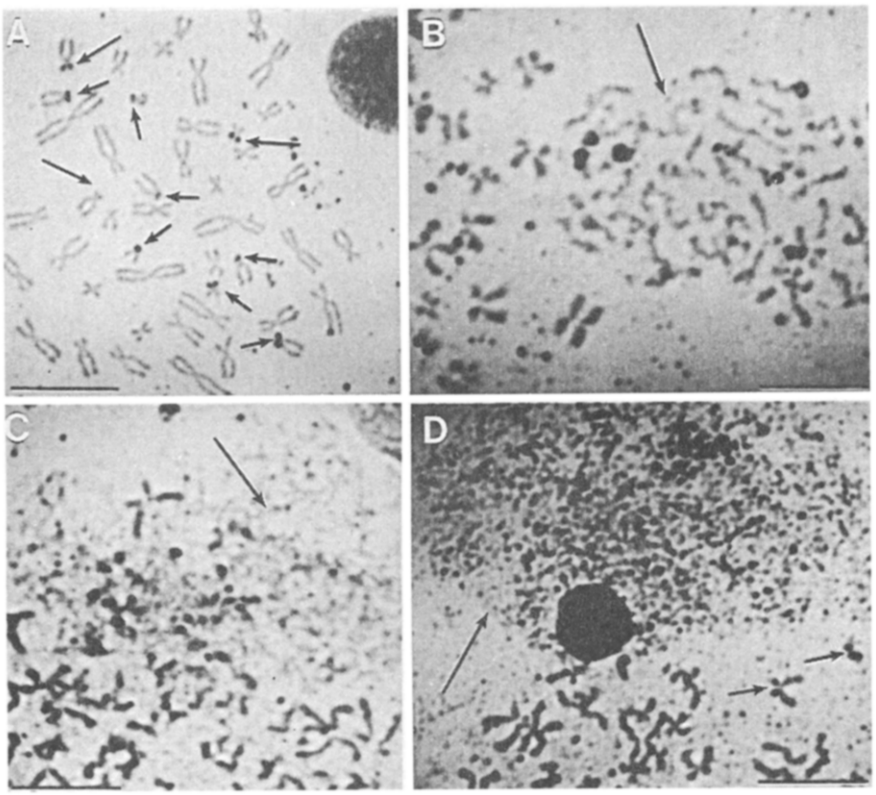

Fig. 1. Chromosome condensability and silver stainability throughout the cell cycle. **A.** Conventional mitotic spread, stained with silver. This panel is a conventional spread of the chromosomes from a mitotic, IMR-90 human diploid fibroblast. It has been stained with silver nitrate to reveal the nucleolar organizer regions (NORS = locations of ribosomal RNA genes) on the short arms of the 10 acrocentric chromosomes, which are shown by the arrows. The size of each silver deposit is a measure of the extent to which ribosomal genes in the respective NOR were transcribed during the previous interphase. The nucleoli in interphase nuclei (upper right-hand corner) are also stained with silver. Silver stainability of the NORs is a measure of one of the variables of the inherited rate model (Y). The bar represents approx. 6 μm. **B–D.** Prematurely condensed chromosomes (PCCs). The chromosomes in interphase nuclei may be forced to condense prematurely by fusing interphase cells with mitotic cells. The degree of condensation is a measure of the cell cycle state of the interphase cell prior to the fusion, and is one of the variables of the inherited rate model (X). Panels B–D show prematurely condensed chromosomes from early G1, late G1 and S phase cells, respectively (long arrows). Each panel also contains the highly condensed chromosomes from the mitotic cell that was used in the fusion. The mitotic chromosomes are more condensed than in panel A due to the use of colcemid as a blocking agent. Each of the spreads is stained with silver nitrate to reveal the location of the NORs. **B.** Prematurely condensed chromosomes from early G1 cells resemble the chromosomes in mitosis, except that they contain a single chromatid. **C.** As G1 progresses, fibers in the PCCs become increasingly dispersed. **D.** PCCs from S phase cells are fragmented, so it is not possible to use their degree of condensation as a measure of cell cycle maturity. Large silver deposits are present in S phase PCCs (as well as in uncondensed, interphase nuclei). This is because the chromosomes are too fragmented for the NORs in nucleoli to separate. The deposit forms rapidly around the cluster of NORs and then grows in proportion to its surface area. For comparison with the large deposit in this panel, silver deposits on the NORs of the mitotic chromosomes are indicated by short arrows. The bar in panels B–D represents approx. 4 μm.

Anatomy of nucleoli

Ribosomal RNA constitutes some 80% of a cell's RNA but is coded by much less than 1% of the cell's DNA, viz. rDNA genes. They are by far the most actively transcribed genes in the nucleus. In human cells, the rDNA is clustered on the short arms of five pairs of chromosomes (Nos 13, 14, 15, 21 and 22) in the nucleolar organizer regions (NORs). As shown in Fig. 1 and as discussed below, these genes may be localized by staining with heavy metals (silver or bismuth). In interphase nuclei, the rDNA genes are located within nucleoli (see Fig. 3), where they are transcribed for the production of ribosomal RNA. Since there are 10 nucleolar organizer regions, a human cell may contain up to 10 nucleoli [75]. Cells ordinarily contain fewer than this maximum number: miniature

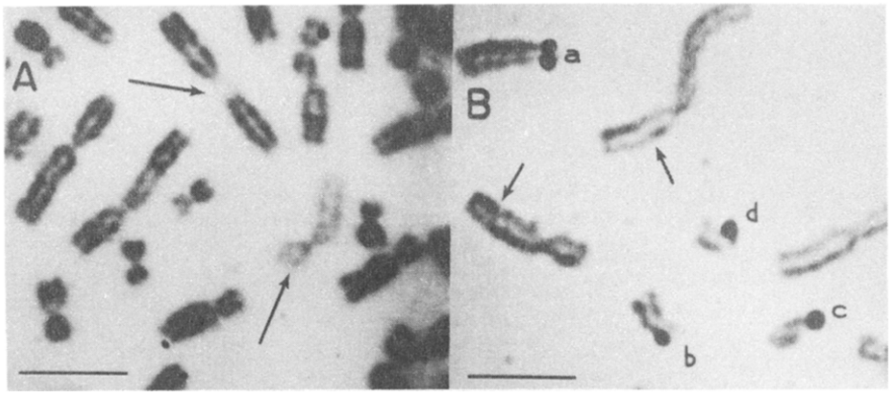

Fig. 2. Use of bromodeoxyuridine as a DNA label. **A**. Late-replicating chromosome regions in IMR-90 human diploid fibroblasts. Cultured fibroblasts were grown in a medium containing thymidine, except for the last 5 h of their lives, when the medium was shifted to one containing bromodeoxyuridine, which is incorporated into DNA in place of thymidine. The cells were harvested in mitosis, and chromosome spreads were prepared. They were then stained with the dye Hoechst 33258, irradiated with u.v. light and stained with Giemsa. The effect is to destroy regions of the chromosomes that had incorporated the bromodeoxyuridine. Two such regions are shown by arrows. One is a centromeric region and the other is a whole chromosome, the inactive X chromosome of this female cell line. Pulse labeling with bromodeoxyuridine at different periods of the S-phase may be used to map the sequence of band replication, which is the model's definition of cell cycle maturity for S phase cells. The bar represents approx. 3 μm. **B**. Asymmetry of silver staining and its relation to new vs old DNA strands. The sister chromatids of the acrocentric chromosomes may exhibit silver deposits of different sizes, indicating that daughter cells will receive NORs that differ in the transcribability of their rDNA genes. Most asymmetric staining is slight, as found by comparing the sister chromatids of the chromosome labeled "a". Highly asymmetric staining exhibited by chromosome "b" is rare. Such staining asymmetry would be important if the silver deposit were systematically larger or smaller on the sister chromatid that contained newer or older DNA strands, respectively, and if all of the newer or older chromatids segregated into one of the daughter cells. To see whether this is the case, these cells were grown in media containing bromodeoxyuridine for one generation and then grown for a second generation in media containing thymidine. Chromosome spreads were then prepared as in panel A. We found no preferential staining of the older (lighter) or newer (darker) chromatids. Highly asymmetric staining may actually be an artifact, for the following reason. Chromosomes may show a single deposit if the sister chromatids lie close to one another, as in chromosome "c". This may happen by chance if the chromosomes are twisted, as in chromosome "d". Sister chromatid exchanges are shown by arrows. The bar represents approx. 2 μm.

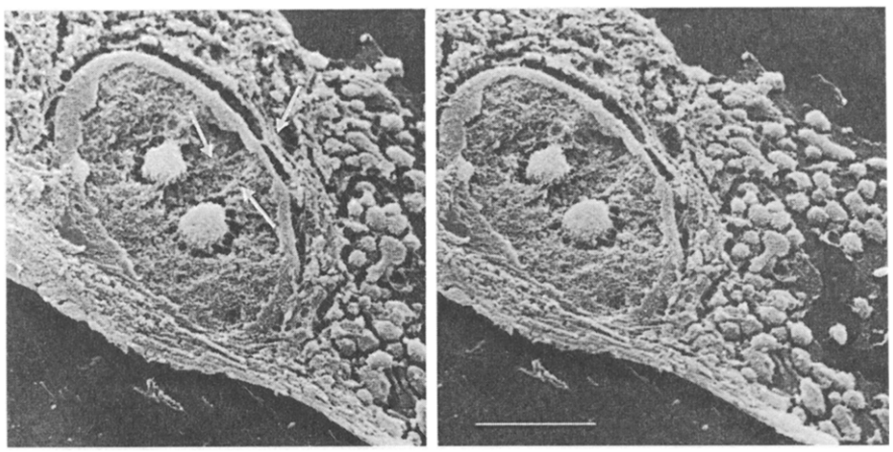

Fig. 3. Nucleolar cables connect cisternae of the endoplasmic reticulum with the nucleolus, through the nuclear envelope. This scanning electron micrograph was prepared by growing IMR-90 fibroblasts on a coverslip, fixing the cells with glutaraldehyde/osmium and then critical-point drying. The upper half of the cell was removed by the lifting of applied adhesive tape, revealing the internal structure of the cytoplasm and nucleus. The two large spherical objects in the nucleus are nucleoli. They are connected directly to the endoplasmic reticulum by cables (arrows), which lie near the lower surface of the nucleus and were exposed by the removal of chromosomes. Proteins used for synthesis in the nucleolus are presumed to enter from the cytoplasm along the cable. The mitochondria that appear as a flock to the right of the nucleus are larger than usual. They often appear as snakes embedded in the endoplasmic reticulum that surrounds the nucleus. The bar represents 8 μm. The tilt angle of the stereo pair is 10°.

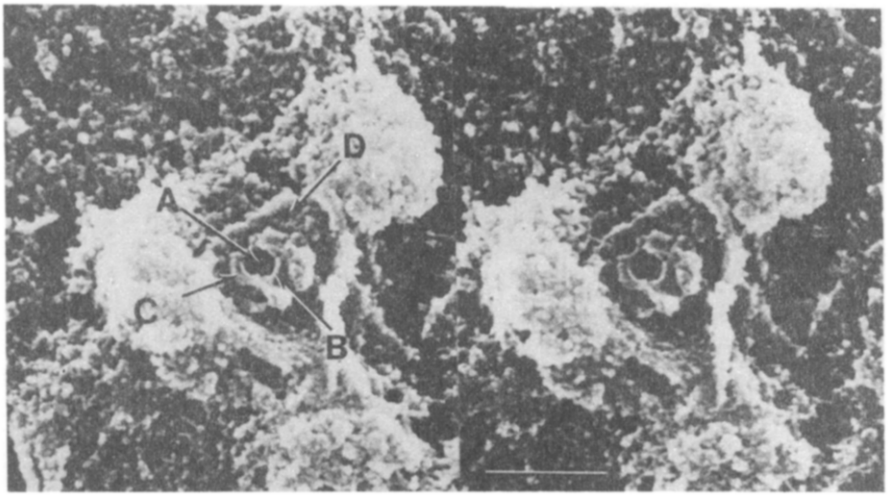

Fig. 4. Fibrillar center of a nucleolus. This scanning electron micrograph was prepared as in Fig. 3. Four nucleoli are in the process of fusing, the central one of which was lifted out of the nucleus along with the upper nuclear envelope. Another fused nucleolus is present in the same nucleus (not shown). The lower portion of the central nucleolus remained attached to its neighbors, allowing some inner components to be visualized. The cup (A) is thought to have contained a cluster of fibrillar centers, collectively termed a fibrillar complex [89]. The shell surrounding the fibrillar complex (B) is thought to be dense fibrillar material, consisting largely of primary rRNA transcripts. The more peripheral material (C) may be the fibrillar component, i.e. rRNA at intermediate stages of processing, which eventually becomes proto-ribosomal subunits in the adjacent granular component (D). The bar represents 1.4 μm. The tilt angle of the stereo pair is 12°.

nucleoli form around the NORs immediately after mitosis, but as time progresses, the nucleoli grow in size and fuse [76, 77]; see Fig. 4. The process reverses as the NORs condense along with all chromosomes during mitosis.

The anatomy of the interphase nucleoli is now understood with reference to the molecular biology of ribosome synthesis, and has been the subject of a number of reviews (molecular aspects, Refs [78–83]; ultrastructural aspects, Refs [84–88]). There are roughly 20 rRNA genes in each of the human NORs, separated from one another by spacer DNA. RNA polymerase I molecules transcribe the genes, producing a 45S ribosomal precursor molecule that is visualized as a branch of the "christmas tree" seen in Miller spreads [84]. The 45S rRNA is subsequently methylated and covered by nucleolar proteins, and is then cleaved and transformed by other nucleolar proteins to produce 28S and 18S ribosomal precursors. The ribosomal subunits are then exported to the endoplasmic reticulum for use in protein synthesis.

The anatomy of nucleoli reflects this series of biochemical events. The exterior of the nucleoli consists largely of ribosomal precursors that are being transported out of the nucleus and are part of the granular component of the nucleolus (Figs 3 and 4). The granular component surrounds (or adjoins) the fibrillar component, which corresponds to rRNA transcripts at intermediate stages of processing. Fibrillar centers (Fig. 4) are situated within the fibrillar component and may be joined in clusters to form a reticulum. The maximum number of fibrillar centers in a diploid cell is roughly equal to the number of rDNA genes, suggesting that the fibrillar centers may be in one-to-one correspondence with the rDNA genes [89]. The view that the shells of the fibrillar centers (dense fibrillar components) are the sites of rRNA transcription is supported by the observation that RNA polymerase I is preferentially located there [90]. Materials that feed the flow of material from the fibrillar centers to the granular component enter the nucleolus through interstices. The interstices may be supplied along cables that connect directly to the endoplasmic reticulum via the nuclear membrane (Fig. 3). Nucleolar feedstocks that must be provided in greatest amount are the proteins that are assembled into the exported ribosomal subunits [91–93]. They are needed at all growth rates since ribosomes in diploid cells have a short half-life [94–96]. Enzymatic components such as RNA polymerase I must also flow into the nucleoli, since the half-life of RNA polymerase I may be as short as 1 [97].

Morphological dynamics of fibrillar centers

Since the fibrillar centers are the structures around which the initial events of ribosome synthesis take place (i.e. rDNA transcription), control over their number and composition is necessarily the first step in regulating the rate of ribosome synthesis. The fibrillar centers and their associated rDNA are in fact the only permanent components of nucleoli. They may also be part of the nuclear matrix, which is preferentially attached to ribosomal DNA [98]. When a cell enters mitosis rRNA synthesis ceases, and the fibrillar and granular components of the nucleoli disappear. The fibrillar centers, however, remain attached to the rDNA even in mitosis and serve as nucleation centers for the subsequent reactivation of nucleoli in the daughter nuclei. Demonstration of the persistence of fibrillar centers is made possible by the fortuitous stainability of one or more of its components with silver [99, 100], i.e. the silver-stained objects in Fig. 1 are actually coalesced fibrillar centers that would also have been stained in interphase. The subject of NOR silver staining has a large literature, a guide to which is provided in the *ISI Atlas of Science* [101]. Unfortunately, the histochemical procedures that make the centers visible cannot be applied to living cells, so that the dynamics of fibrillar center formation and disappearance has not been studied directly. Inferences concerning their dynamics must be made from populations of fixed cells, through light and electron microscopy. Fibrillar centers that are stained with Toluidene Blue were known by the classical cytologists as nucleolini. They are too numerous to count and too small to resolve clearly by light microscopy, but it is possible to determine that within individual nucleoli of diploid cells, they have roughly the same size under conditions that favor cell proliferation [102–104]. The number and morphology of fibrillar centers have also been studied by examining electron micrographs of serial and random sections of nucleoli [89, 105–107]. The studies demonstrate that the morphology of fibrillar centers depends on the type of cell under investigation and the conditions of their growth. However, for diploid cells, generalizations from the studies are that the number of fibrillar centers is greatly in excess of the number of NORs, varies considerably among cells in the same population and increases with increasing levels of rRNA synthesis. This variability in the number of fibrillar centers is accompanied by cell-to-cell variability in the degree of silver staining of NORs and by increased staining as the rate of rRNA syntheis increases [108–111].

Biochemical dynamics of fibrillar centers

Biochemical studies concerning the control of nucleolar activity have considered both the long-term inactivation of rDNA genes and short-term changes in function [112]. Long-term inactivation of rRNA genes, especially those that have been amplified in number to excess, may be accomplished by methylation [113]. Control of rDNA genes that occurs over a time span comparable to a single cell generation has been studied by Busch and his colleagues [114–116]. When nucleolar proteins were examined under conditions in which rRNA synthesis was stimulated to high levels, it was observed that one nucleolar protein (A24) decreased markedly. The protein was subsequently shown to be ubiquitinated histone 2A (Ub-2A). On first inspection, this observation is surprising, since transcriptionally active chromatin contains ubiquitinated nucleosomes, and transcriptionally inactive chromatin does not contain significant levels of Ub-2A [117–119]. The explanation for the absence of Ub-2A from highly active rDNA appears to be that in progressing from moderate, reversible levels of transcription [120] to high levels of transcription, (ubiquitinated) nucleosomes are displaced from the rDNA [121]. Evidently, they are replaced by transcriptional complexes analogous to those associated with the activation of 5s RNA [122, 123] components of which constitute the fibrillar center and which preferentially stain with silver (Fig. 1). Conversely, the suppression of rDNA transcription results in a reduction or suppression of silver staining (number of fibrillar centers), as has been documented in somatic cell hybrid systems [124–126] and in slowly growing fibroblasts [109]. Thus, it appears that the (variable) degree of fibrillar center silver staining is a measure of the extent to which a cell's rDNA has made the transition from inactivation (methylation) to modest transcription (ubiquitinated nucleosomes) to a high level of transcriptional activity (nucleosomal displacement; fibrillar center formation).

C. The Relation Between Cell Cycle and Nucleolar Activity

The involvement of Ub-2A in the control of rRNA synthesis is relevant to the definition of the

cell cycle in terms of chromatin condensation. This semihistone is essentially the only structural polypeptide that is present throughout interphase chromatin, but that is absent from condensed, mitotic chromatin [119]. It is thought that the presence of Ub-2A affects the flexibility of adjacent nucleosomes, thereby inhibiting chromatin condensation [127, 128]. Although large-scale structures involving the nuclear envelope [129] as well as dehydration by inorganic cations and polyamines, H1 phosphorylation, methylation and poly(ADP)ribosylation may also influence the degree of chromatin condensation [130], the participation of ubiquitin is most important in the present context: chromatin decondensation increases in G1 when the chromosomes become ubiquitinated, and condensation increases in G2 as the ubiquitin is removed, leading to the condensed mitotic chromosome that is free of ubiquitin.

Ubiquitin provides a mechanism relating chromatin condensation (cell cycle progress) to the control of protein turnover [97, 131–134] and to the expresion not only of ribosomal genes, but of genes throughout the nucleus [116–118, 133, 135, 136]. Ubiquitin is a small protein that is conjugated to other proteins, serving as a signal for attack by ATP-dependent proteases that are specific for ubiquitin–protein conjugates. Varshavsky, Levinger and colleagues have developed the proposition that ubiquitin-dependent proteolysis of histones is a general mechanism for exposing chromatin that is to be made accessible for transcription, brought about by the removal of histones. In particular, the Ub-2A in the nucleosomes attached to rDNA may be attacked, making the rDNA available for the transcriptional machinery of fibrillar centers.

The proposed mechanism relating the rate of cell cycle progress to the level of nucleolar activity is as follows. A large percentage of the material that enters the nucleus is thought to pass through the nucleoli along routes that connect the cytoplasm to nucleoli, as shown in Fig. 3. The fibrillar centers are a bottleneck in this flow of material and serve to control it. Enzymatic components of the ubiquitin system are present in the flow, and fluctuations in their concentration cause the number of fibrillar centers to increase and decrease episodically, modulating the rate of ribosome synthesis both through the number of transcribable rDNA genes and through the rate at which nucleolar precursors are made available from the cytoplasm. The rate of flow of components of the ubiquitin protein turnover system also influences the rate of chromosome decondensation and recondensation, through the mechanisms mentioned above.

This model relates the capacity to make ribosomes (number of fibrillar centers) to the rate at which a cell progresses through the cell cycle. If the number of fibrillar centers is rate-limiting, the capacity to make ribosomes will also be proportional to the rate at which ribosomes are actually synthesized, so mitotic activity will increase as the rate of ribosome synthesis increases [137, 138]. However, ribosome synthesis *per se* is not considered to be the cause of cell cycle progression—the cause is the flow of material from the cytoplasm to the nucleus (that is directed towards the fibrillar centers), some of which causes cell cycle maturation. Evidently, ribosome synthesis is not required for cell cycle progress since rRNA synthesis decreases in G2 and comes to a halt in mitosis, while the cell cycle continues. Thus, the model is consistent with the dissociability of ribosome synthesis and cell cycle progress [139–141], so long as lack of ribosome synthesis is not due to congestion in the flow of cell cycle related material into the nucleus. The details of the reactions involved and the way in which the cell's protein turnover machinery is controlled by the growth conditions are beyond the scope of the model in its present form. It should be noted, though, that the two growth factors that have the greatest influence on the rate of fibroblast proliferation, namely, epidermal growth factor and insulin-like factors [142–144] have a pronounced and immediate effect on the biochemistry of ribosomal subunits [145–148] and could therefore participate in the control of their activity and turnover.

3. FORMULATION OF THE MODEL

A. Specification of the Transitions

Let the state of a human, diploid cell be denoted by a random vector $(X, Y_1, Y_2, \ldots, Y_{10})$, where X represents the cell cycle state and Y_i represent the number of fibrillar centers associated the ith NOR in a cell. We assume that there is one fibrillar center per activated rDNA gene. In order to formulate the model, we must specify the way in which the state of the cell may change throughout

the cell cycle, including consideration of whether the number of fibrillar centers changes when the rDNA genes are duplicated. As described in the previous section, the variable X is used to represent successive stages of cell cycle maturation (degree of chromatin condensation for G1 and G2 cells, stage of band replication for cells in the S phase). Its value is defined to equal zero for a newly-formed cell and X_{max} for a cell that is in the process of dividing. The conventional chromosome replication cycle G1, S, G2 and M may be defined by dividing the range of maturation states (0 to X_{max}) into successive blocks. Cell cycle progression is assumed to be irreversible, so that X can only increase (or remain constant) with increasing cell age. Furthermore, X is defined to be an integer. A continuous progression along the cell cycle [52–55] is treated as a limiting case in which $X_{max} \to \infty$. As discussed in the previous section, the rate of cell cycle progression is thought to be correlated with the number of fibrillar centers in a cell. We will assume that the probability per unit time of cell cycle progress is linearly proportional to the number of fibrillar centers (silver stainability), which is in turn proportional to the number of activated ribosomal genes. Thus, the average rate of cell cycle progress is proportional to the number of fibrillar centers.

The simplest view of rDNA transcription is that each of the rDNA genes in a cell at any instant is either on (displaced nucleosomes) or off, with no intermediate level of activity. The state of each nucleolar organizer is defined as the sum of the number of its active rDNA genes and will therefore have some value between zero and the total number of rDNA genes in that NOR. It must then be decided whether to assume that all rDNA genes in an NOR become activated and inactivated in unison or whether the rDNA genes in a NOR undergo transitions independently of one another. If the former possibility is correct, then the Y_i are binary variables, and if the latter is correct, we consider the possibility that there are up to 200 independent rDNA transcriptional centers in the nucleus. Both cases are covered if we simply assume that there is a finite number of independent transcriptional centers in the nucleus (Y_{max}), and allow this number to vary between 10 and 200 in any simulations that are performed.

A final consideration is whether to allow the number of possible transcriptional centers to double when the rDNA genes are duplicated. After duplication, the potential rate of rRNA synthesis doubles [149, p. 180], but the question is whether the sister genes separate during the remainder of the cell cycle to become independent centers or whether they remain adjacent to one another until mitotic condensation forces the sister chromatids to separate. The significance of the autonomy depends on whether the replication of the rDNA genes occurs early or late in the cell cycle: if the genes are replicated late, they will have little time to separate, even if it is possible for them to do so. The timing of rDNA replication may be independent of that of other genes [150], which may explain the observation of early, late and variable rDNA replication in different cell types [151–161]. In the absence of information about the movements of sister rDNA genes as they course though the nucleoli, we will adopt the simplest model, namely, that the sister rDNA genes remain associated with one another and become transcribed or inactive in unison, eventually separating in G2 as they condense for mitosis.

As described in the previous section, the transcriptional potential of the ribosomal genes is maintained throughout mitosis by the persistence of the fibrillar centers, so the transcriptional state of the mother cell is passed to its daughter cells. Sister chromatids are usually symmetric with regard to their silver staining (Figs 1 and 2), so the daughter nuclei are assumed to receive equivalent fibrillar centers from a given chromosome. Varying degrees of asymmetric staining of sister chromatids are occasionaly observed (Fig. 2) and may contribute to differences between the cell cycle kinetics of sibling cells. For the present purposes, however, any asymmetry will be ignored as a secondary phenomenon. In order to treat it properly, we would be obliged to make a large number of assumptions concerning the origin of this asymmetry and concerning the mechanics of chromosome segregation [162–166]. Instead, we will assume that the number of fibrillar centers in each newly-formed daughter cell is the same as the number present in the mitotic mother cell.

To summarize the model, our assumptions concerning the existence of independent transcriptional centers and their persistence during rDNA duplication and mitosis allow us to simplify the definition of the state of a cell to a random vector (X, Y), where X is the cell cycle state and Y is the total number of independent transcriptional centers. For the purpose of analysis, Y will be considered equal to the number of fibrillar centers, in excess of the number found in a quiescent

cell. Then, the transitions that are allowed by the model are as follows:

Transition	Probability per unit time	Event	
$(X, Y) \rightarrow (X+1, Y)$	βY	Cell cycle progression	(1a)
$(X_{max}, Y) \rightarrow (0, Y) + (0, Y)$	βY	Cell division	(1b)
$(X, Y) \rightarrow (X, Y+1)$	$\lambda(Y_{max} - Y)$	rDNA gene activation	(1c)
$(X, Y) \rightarrow (X, Y-1)$	μY	rDNA gene inactivation	(1d)

Note that the model contains three primary parameters: β (probability per unit time of cell cycle progression per active gene); λ (probability per unit time of gene activation per inactive gene); and μ (probability per unit time of gene inactivation per active gene). Over any small time interval ΔT, the probabilities of each of the above transitions are $\beta Y \Delta T$, $\lambda(Y_{max} - Y)\Delta T$, and $\mu Y \Delta T$, respectively. The probability of two transitions over the same interval ΔT is the product of the probabilities of the individual transitions, so in the limit that $\Delta T \rightarrow 0$, we may ignore the possibility of two or more transitions.

B. Calculations that Follow

The model may be used to simulate three types of experiments. The first is one in which the cell-to-cell distribution of cell properties is measured. The property might be DNA content, whose distribution among the cells of a population can be measured by flow cytometry. Another property is the number of fibrillar centers in a cell, measured as the size of silver deposits on each of the 10 NORs of a chromosome spread. If only a single distribution is measured, it is ordinarily assumed that this distribution corresponds to an exponentially growing ("steady state") population. The second type of experiment is the time-lapse microcinematography of proliferating cells, which provides information concerning the distribution of cell generation times, including the relation between the generation times of sibling and mother–daughter pairs. The third type of experiment is the response of a cell population to some change in growth conditions. The most common procedure is to label S phase cells of an exponentially growing population and to then measure the fraction of labeled mitotic cells at a series of subsequent time points.

The analysis of the inherited rate model will be presented in an order corresponding to these three types of experiments. In the next section, the distribution of cell properties (X and Y) will be calculated as a function of the model's parameters. Knowledge of this distribution is a prerequisite for interpreting the dispersion of generation times measured by time-lapse microcinematography, for the following reason. Since the rate of cell cycle progress depends on the number of fibrillar centers, a cell will progress through the cell cycle at a rate that is conditioned by the (variable) number of fibrillar centers that it inherited. This conditional generation time will be examined in Section 5. Compounding the cells' distribution in the initial number of fibrillar centers with the distribution of generation times (among cells that start their lives with a particular number of fibrillar centers), gives the cumulative distribution of cell generation times that may be compared with time-lapse microcinematography data. This compound distribution is examined in Section 6. The problem of correlations between the generation times of related cells is also examined there. These distributions refer to cells of a population that is growing exponentially. The growth of populations that are not initially in the "steady state" is investigated in Section 7. Such populations more or less rapidly re-achieve "steady state" growth, exhibiting damped oscillations as they evolve. Finally, the growth of a cell population that is subjected to periodic perturbation is considered in Section 8. This situation corresponds to cells that are exposed periodically to cytotoxic agents.

4. DISTRIBUTION OF CELL PROPERTIES IN A "STEADY STATE" POPULATION

A. Rate Equations

Equations (1a–d) define a stochastic model of cell proliferation. However, if the size of the population is large, stochastic aspects of population growth may be ignored, and the population

may be described by deterministic equations. The fundamental equation of population growth is a stochastic master equation, and the deterministic equations are obtained by averaging the master equation. The procedure for doing so is discussed in Appendix A. Note that although the deterministic equations may also be constructed by inspection of the allowed transitions (1a–d), this is not always a legitimate procedure [167, 168], and Appendix A provides the justification for this particular model.

Let $N(x, y; t)$ denote the expected number of cells in each state at time t. Then according to the transitions allowed by equations (1a–d), the $N(x, y; t)$ satisfy the differential equations

$$\frac{d}{dt}N(0, y; t) = 2\beta y N(X_{max}, y) + \lambda[Y_{max} - (y-1)]N(0, y-1) + \mu(y+1)N(0, y+1) - [\beta y + \lambda(Y_{max} - y) + \mu y]N(0, y) \tag{2a}$$

and

$$\frac{d}{dt}N(x, y; t) = \beta y N(x-1, y) + \lambda[Y_{max} - (y-1)]N(x, y-1) + \mu(y+1)N(x, y+1) - [\beta y + \lambda(Y_{max} - y) + \mu y]N(x, y), \tag{2b}$$

where equation (2b) holds for $x = 1, 2, \ldots, X_{max}$. Note that these equations cover all combinations of x and y, provided that we define $N(x, y; t = 0) = 0$ for $y > Y_{max}$ and for $y < 0$.

The expected total number of cells is

$$N_{tot}(t) = \sum_{x=0}^{X_{max}} \sum_{y=0}^{Y_{max}} N(x, y; t) \tag{3}$$

which increases in time as

$$\frac{d}{dt}N_{tot}(t) = \sum_{y=0}^{Y_{max}} \beta y N(X_{max}, y; t). \tag{4}$$

Let $f(x, y; t)$ denote the expected fraction of cells in each of the (X, Y) states:

$$f(x, y; t) = \frac{N(x, y; t)}{N_{tot}(t)}. \tag{5}$$

Then,

$$\frac{d}{dt}f(x, y; t) = \frac{\frac{d}{dt}N(x, y)}{N_{tot}} - \frac{N(x, y)}{N_{tot}} \cdot \frac{\frac{d}{dt}N_{tot}}{N_{tot}}, \tag{6a}$$

$$\frac{d}{dt}f(0, y; t) = 2\beta y f(X_{max}, y) + \lambda[Y_{max} - (y-1)]f(0, y-1) + \mu(y+1)f(0, y+1) - [\beta y + \lambda(Y_{max} - y) + \mu y + k(t)]f(0, y), \tag{6b}$$

$$\frac{d}{dt}f(x, y; t) = \beta y f(x-1, y) + \lambda[Y_{max} - (y-1)]f(x, y-1) + \mu(y+1)f(x, y+1) - [\beta y + \lambda(Y_{max} - y) + \mu y + k(t)]f(x, y) \tag{6c}$$

and

$$N_{tot}(t) = N_{tot}(0)\exp\left[\int_0^t dt' k(t')\right], \tag{7a}$$

where

$$k(t) = \frac{\frac{d}{dt}N_{tot}(t)}{N_{tot}(t)} = \sum_{y=0}^{Y_{max}} \beta y f(X_{max}, y; t). \tag{7b}$$

B. Malthusian Parameter and the Distribution of Cell Properties

As discussed in Appendix D, equations (6a–c) exhibit an equilibrium point that is obtained for large time, irrespective of the initial state of the population. To find the asymptotic fractions, we may either solve equations (6a–c) with the time derivatives set equal to zero or may make use of equations (2a, b): for large time, each of the $N(x, y; t)$ grows as $N(x, y; t) \sim f(x, y; \infty)\exp(kt)$, where $f(x, y; \infty)$ is the asymptotic fraction and k is the Malthusian parameter of exponential growth. Substituting this expression into equations (2a, b), we obtain the following eigenvalue equations for the Malthusian parameter:

$$kf(0, y; \infty) = 2\beta y f(X_{\max}, y; \infty) + \lambda[Y_{\max} - (y-1)]f(0, y-1; \infty) + \mu(y+1)f(0, y+1; \infty) - [\beta y + \lambda(Y_{\max} - y) + \mu y]f(0, y; \infty) \tag{8a}$$

and

$$kf(x, y; \infty) = \beta y f(x-1, y; \infty) + \lambda[Y_{\max} - (y-1)]f(x, y-1; \infty) + \mu(y+1)f(x, y+1; \infty) - [\beta y + \lambda(Y_{\max} - y) + \mu y]f(x, y; \infty). \tag{8b}$$

Since the expected distribution of active rDNA genes is the same for mother and daughter cells and since the gene transitions are not explicit functions of the value of X, $f(x, y; \infty)$ will factorize as

$$f(x, y; \infty) = f(x, \cdot\,; \infty) f(\cdot\,, y; \infty). \tag{9}$$

Summation of equations (8a, b) over y provides the following expressions for $f(x, \cdot\,; \infty)$:

$$f(0, \cdot\,; \infty) = \frac{2\beta\langle Y\rangle}{k + \beta\langle Y\rangle} f(X_{\max}, \cdot\,; \infty) \tag{10a}$$

and

$$f(x, \cdot\,; \infty) = \frac{\beta\langle Y\rangle}{k + \beta\langle Y\rangle} f(x-1, \cdot\,; \infty), \tag{10b}$$

where

$$\langle Y\rangle = \sum_{y=0}^{Y_{\max}} y f(\cdot\,, y; \infty). \tag{10c}$$

Then the $f(x, \cdot\,; \infty)$ are found to equal

$$f(x, \cdot\,; \infty) = 2(1 - \Omega)\Omega^x, \tag{11a}$$

where

$$\Omega = \left(\frac{1}{2}\right)^{1/(X_{\max}+1)} = \frac{\beta\langle Y\rangle}{k + \beta\langle Y\rangle}. \tag{11b}$$

Substituting equations (9) and (11a, b) into equations (8a, b), we find that for the exponentially growing population, the $f(\cdot\,, y; \infty)$ satisfy the eigenvalue equation

$$kf(\cdot\,, y; \infty) = \frac{\beta y}{\Omega} f(\cdot\,, y; \infty) + \lambda[Y_{\max} - (y-1)]f(\cdot\,, y-1; \infty) + \mu(y+1)f(\cdot\,, y+1; \infty) - [\beta y + \lambda(Y_{\max} - y) + \mu y]f(\cdot\,, y; \infty). \tag{12}$$

The solution to this equation provides both the Malthusian parameter (k) and the distribution in the number of fibrillar centers, $f(\cdot\,, y; \infty)$, as a function of the model's parameters. The method for solving it is presented in Appendix B.

Once the "steady state" distribution of X and Y is known, it is useful to express equations (6b, c) in terms of the deviation from these asymptotic values. The following equations will be used later

to calculate fraction-labeled-mitoses curves and to analyze the stability properties of the model:

$$\Delta f(x, y; t) = f(x, y; t) - f(x, y; \infty), \tag{13}$$

$$\begin{aligned}\frac{\mathrm{d}}{\mathrm{d}t}\Delta f(0, y; t) = {} & 2\beta y \Delta f(X_{\max}, y) + \lambda[Y_{\max} - (y-1)]\Delta f(0, y-1) \\ & + \mu(y+1)\Delta f(0, y+1) - [\beta y + \lambda(Y_{\max} - y) + \mu y + k]\Delta f(0, y) \\ & - f(0, y; \infty)\Delta k(t) - [\Delta f(0, y)][\Delta k(t)],\end{aligned} \tag{14a}$$

$$\begin{aligned}\frac{\mathrm{d}}{\mathrm{d}t}\Delta f(x, y; t) = {} & \beta y \Delta f(x-1, y) + \lambda[Y_{\max} - (y-1)]\Delta f(x, y-1) \\ & + \mu(y+1)\Delta f(x, y+1) - [\beta y + \lambda(Y_{\max} - y) + \mu y + k]\Delta f(x, y) \\ & - f(x, y; \infty)\Delta k(t) - [\Delta f(x, y)][\Delta k(t)]\end{aligned} \tag{14b}$$

and

$$N_{\text{tot}}(t) = N_{\text{tot}}(0)\exp\left[kt + \int_0^t \mathrm{d}t' \Delta k(t')\right], \tag{15a}$$

where

$$\Delta k(t) = \sum_{y=0}^{Y_{\max}} \beta y \Delta f(X_{\max}, y; t). \tag{15b}$$

5. DISTRIBUTION OF GENERATION TIMES FOR GIVEN INITIAL CONDITIONS

A. Master Equation for a Single Cell

The model given in equations (1a–d) implies the following master equation for the probability that a cell be in the state $(X, Y) = (x, y)$ at age a, given that its initial state was $(X, Y) = (0, y_0)$. Let $P(x, y; a, y_0)$ denote this probability, conditional on the indicated initial value of Y:

$$\begin{aligned}\frac{\mathrm{d}}{\mathrm{d}a}P(x, y; a, y_0) = {} & \beta y P(x-1, y) + \mu(y+1)P(x, y+1) \\ & + \lambda[Y_{\max} - (y-1)]P(x, y-1) - [\beta y + \lambda(Y_{\max} - y) + \mu y]P(x, y).\end{aligned} \tag{16}$$

If $x > X_{\max}$, it is understood that the cell has divided, i.e. the (random) time required for the cell to divide is the time required for it to reach the "state" $X_{\max} + 1$. To solve these coupled differential equations, we will make use of the generating function for $P(x, y; a, y_0)$, which is defined as

$$G(u, v; a, y_0) = \sum_{x=0}^{X_{\max}} \sum_{y=0}^{Y_{\max}} P(x, y; a, y_0) u^x v^y. \tag{17}$$

If the generating function is known, the distribution may be recovered by expanding G in powers of u and v and by picking out the coefficients, or by using the expression

$$P(x, y; a, y_0) = \frac{1}{x!y!}\frac{\partial^x}{\partial u^x}\frac{\partial^y}{\partial v^y} G(u, v; a, y_0)\Big|_{\substack{u=0 \\ v=0}}. \tag{18}$$

B. Generating Function for the Solution of the Master Equation

Since the transition rates given in equations (1a–d) are linear in Y, the random vector (X, Y) may be decomposed into the sum of $Y_{\max}$ independent random vectors, each of which corresponds to a solution of the master equation. For the case $Y_{\max} = 1$, equation (16) becomes

$$\frac{\mathrm{d}}{\mathrm{d}a}P(x, 0; a, y_0, Y_{\max} = 1) = -\lambda P(x, 0) + \mu P(x, 1), \tag{19a}$$

$$\frac{\mathrm{d}}{\mathrm{d}a}P(x, 1; a, y_0, Y_{\max} = 1) = \lambda P(x, 0) - \mu P(x, 1) + \beta P(x-1, 1) - \beta P(x, 1). \tag{19b}$$

If we multiply equations (19a, b) by u^x and then sum over x, we obtain an equivalent expression in terms of the generating function. Let

$$G(u, v; \boldsymbol{a}, y_0, Y_{\max} = 1) = c(u; \boldsymbol{a}, y_0) + v\, d(u; \boldsymbol{a}, y_0),$$

$$c(u; \boldsymbol{a}, y_0) = \sum_{x=0}^{\infty} P(x, 0; \boldsymbol{a}, y_0) u^x,$$

$$d(u; \boldsymbol{a}, y_0) = \sum_{x=0}^{\infty} P(x, 1; \boldsymbol{a}, y_0) u^x, \tag{20a}$$

then equations (19a, b) imply that

$$\frac{\mathrm{d}}{\mathrm{d}\boldsymbol{a}} c(u) = -\lambda c(u) + \mu d(u),$$

$$\frac{\mathrm{d}}{\mathrm{d}\boldsymbol{a}} d(u) = \lambda c(u) - [\mu - \beta(u-1)] d(u). \tag{20b}$$

Equations (20a, b) may be solved using Laplace transforms and have the following solutions for the two initial conditions $y_0 = 0$ and $y_0 = 1$:

$$G(r_{\pm}(u), v; \boldsymbol{a}, 0, Y_{\max} = 1) = \left[1 + \frac{\lambda\mu}{(r_+ + \lambda)(r_- + \lambda)}\right] \exp(-\lambda \boldsymbol{a}) + \left(\frac{\lambda\mu}{r_+ + \lambda} + \lambda v\right) \frac{\exp(\boldsymbol{a} r_+)}{r_+ - r_-} + \left(\frac{\lambda\mu}{r_- + \lambda} + \lambda v\right) \frac{\exp(\boldsymbol{a} r_-)}{r_- - r_+} \tag{21a}$$

and

$$G(r_{\pm}(u), v; \boldsymbol{a}, 1, Y_{\max} = 1) = [\mu + (\lambda + r_+)v] \frac{\exp(\boldsymbol{a} r_+)}{r_+ - r_-} + [\mu + (\lambda + r_-)v] \frac{\exp(\boldsymbol{a} r_-)}{r_- - r_+}, \tag{21b}$$

where u enters only through $r_{\pm}$, which are the solutions to the quadratic equation

$$s^2 + [\lambda + \mu - \beta(u-1)]s - \lambda\beta(u-1) \equiv (s - r_+)(s - r_-) = 0, \tag{22a}$$

namely,

$$r_{\pm}(u) = \tfrac{1}{2}\{-[\lambda + \mu - \beta(u-1)] \pm \{[\lambda + \mu - \beta(u-1)]^2 + 4\beta\lambda(u-1)\}^{1/2}\}. \tag{22b}$$

Now consider the problem when $Y_{\max}$ is some arbitrary integer >1. If the cell initially contains y_0 active rDNA genes, the generating function as a function of age is simply the product of the generating functions associated with the individual genes [e.g. 169]:

$$G(u, v; \boldsymbol{a}, y_0, Y_{\max} \neq 1) = [G(r_{\pm}(u), v; \boldsymbol{a}, 0, Y_{\max} = 1)]^{Y_{\max} - y_0} [G(r_{\pm}(u), v; \boldsymbol{a}, 1, Y_{\max} = 1]^{y_0}. \tag{23}$$

The problem of determining the distribution of generation times for a given initial condition is essentially solved, since we know the generating function given by equation (23), which may be inverted using equation (18). This first passage time problem may be carried through analytically and is presented in Appendix C. Without going into details, it is possible to gain a feeling for the way in which the distribution changes as a function of the model's parameters. Note that if we let $u = 1$, then $r_+ = 0$ and $r_- = -(\lambda + \mu)$, and equation (23) provides the generating function for the value of Y at age $\boldsymbol{a}$, irrespective of the value of X:

$$G(1, v; \boldsymbol{a}, y_0) = \left[1 + \frac{\lambda}{\lambda + \mu}(v-1)\{1 - \exp[-(\lambda + \mu)\boldsymbol{a}]\}\right]^{Y_{\max} - y_0} \times \left[1 + (v-1)\exp[-(\lambda + \mu)\boldsymbol{a}] + \frac{\lambda}{\lambda + \mu}(v-1)\{1 - \exp[-(\lambda + \mu)\boldsymbol{a}]\}\right]^{y_0}. \tag{24a}$$

The asymptotic value of this equation is

$$G(1, v; \infty, y_0) = \left[1 + \frac{\lambda}{\lambda + \mu}(v-1)\right]^{Y_{\max}}, \tag{24b}$$

which is the generating function for a binomial distribution with mean value $\lambda Y_{max}/(\lambda + \mu)$. Consequently, in the limit that the parameters λ and μ are much larger than β, Y relaxes rapidly to this binomial distribution. If that is the case, then summing equation (16) over y implies a simple birth process for X, in which the transition rates involving Y are replaced by the expected value of the binomial. That is to say, the expected value of Y would be the same $\forall X$, X would be a Poisson random variable with mean value $\beta\lambda \boldsymbol{a} Y_{max}/(\lambda + \mu)$, and the distribution of cell generation times would be a gamma distribution with mean value $(X_{max} + 1)(\lambda + \mu)/(\beta\lambda Y_{max})$ and variance $(X_{max} + 1)(\lambda + \mu)^2/(\beta\lambda Y_{max})^2$, Refs [170–172]. However, this would also mean that the correlation between the generation times of sibling cells and between mother and daughter cells would be zero. Therefore, the existence of positive correlations between the intermitotic times of related cells constrains the value of β/X_{max} to an order of magnitude that is comparable to that of λ and μ.

6. COMPOUNDED DISTRIBUTION OF GENERATION TIMES IN THE "STEADY STATE"

A. Ambiguity of the Term "Distribution of Generation Times"

Let $A(y_0)$ be the (random) age at which a cell divides, given that it contained y_0 fibrillar centers when it was formed. Then

$$\text{Prob}[A(y_0) < \boldsymbol{a}] = 1 - \sum_{x=0}^{X_{max}} \sum_{y=0}^{Y_{max}} P(x, y; \boldsymbol{a}, y_0), \tag{25}$$

where $P(x, y; \boldsymbol{a}, y_0)$ satisfies equation (16). We define the compounded distribution of cell generation times in a "steady state" population to be

$$\text{Prob}[A < \boldsymbol{a}] = \sum_{y_0=0}^{Y_{max}} f(\cdot, y_0; \infty)\, \text{Prob}[A(y_0) < \boldsymbol{a}], \tag{26}$$

where A is the (random) generation time, irrespective of the initial value of Y. This definition of the distribution of generation times deserves some comment. It corresponds to the following type of experiment. Mitotic cells are selected from an exponentially growing population and are seeded for observation by time-lapse microcinematography or related procedures [26]. Then, equation (26) describes the distribution of generation times among the mitotic cells' daughters (provided that the mitotic cells divide immediately). It has been called the forward distribution of generation times because it looks forward to the ages when newly-formed cells will divide. It is different from the distribution of generation times corresponding to other subpopulations of cells [173]. As examples, distributions of generation times have been defined for the following subpopulations. The distribution corresponding to the subpopulation of cells in the process of division is found by running the clock backward to the times of their formation and therefore is called the backward distribution. Similarly, if we select cells at random from an exponentially growing population (irrespective of whether the cells are newly-formed, dividing or anywhere in between), these cells' generation times are found by running the clock back to the times of their formation and forward to the times of their division. Macdonald [174, 175] called this the "sideways" distribution and analyzed the problem of predicting one of the above distributions from another. "Artificial" vs "real" distributions have also been defined [176, 177] and will be discussed below. The distinction between the various distributions is of interest not only because of the ambiguities that they raise, but more importantly because time-lapse microcinematography data are ordinarily constructed by pooling the generation times corresponding to different subpopulations of cells, i.e. cells of different generations. This point is considered below in connection with the difference between "real" and "artificial" distributions.

B. Comparison of Related Cells

The inherited rate model explains the positive correlations between the intermitotic times of sibling cells as the result of the fact that both siblings inherit the same number of fibrillar centers and that the inheritance varies from sibling pair to sibling pair. Let A_1 and A_2 denote the (random)

generation times of a sibling pair. The joint distribution for A_1 and A_2 is an extension of equation (26):

$$\text{Prob}[A_1 < a_1, A_2 < a_2] = \sum_{y_0=0}^{Y_{max}} f(\cdot, y_0; \infty)\,\text{Prob}[A(y_0) < a_1]\,\text{Prob}[A(y_0) < a_2]. \tag{27}$$

The joint distribution of mother and daughter intermitotic times is a more complicated expression. Let $A_m(y_0 \to y_{X_{max}+1})$ denote the (random) age of division among mother cells that begin their lives with y_0 fibrillar centers and divide with $y_{X_{max}+1}$ fibrillar centers. Let $\Pi(y_0 \to y_{X_{max}+1})$ be the probability that a cell divides with $y_{X_{max}+1}$ fibrillar centers, given that it started with y_0 fibrillar centers [see equation (C.8)]. Let $A_{S1}(y)$ and $A_{S2}(y)$ be the (random) generation times of daughter cells that initially contain y centers. Then, we define the joint distribution of mother and daughter generation times as follows:

$$\begin{aligned}&\text{Prob}[A_m < a_m, A_{S1} < a_{S1}, A_{S2} < a_{S2}]\\ &= \sum_{y_0=0}^{Y_{max}} f(\cdot, y_0; \infty) \sum_{y_{X_{max}+1}=0}^{Y_{max}} \Pi(y_0 \to y_{X_{max}+1})\,\text{Prob}[A_m(y_0 \to y_{X_{max}+1}) < a_m]\\ &\quad \times \text{Prob}[A_{S1}(y_{X_{max}+1}) < a_{S1}]\,\text{Prob}[A_{S2}(y_{X_{max}+1}) < a_{S2}].\end{aligned} \tag{28}$$

Correlations between sibling and mother–daughter generation times are found after averaging equations (25)–(28) over the ages. Expressions needed for the construction of these averages are provided in Appendix C.

Note the following points concerning the distributions that are defined by equations (27) and (28):

(i) By analogy with the discussion surrounding the definition of cell generation times, these distributions should be called the forward joint distributions of sibling and mother–daughter pairs.

(ii) The population doubling time is not equal to either the average mother or the average daughter generation time (found by integrating $1 - \text{Prob}(A < a)$ over a, $0 < a < \infty$, for either of the random age variables). For example, in the gamma function limit [see equation (24b)], the population doubling time is $\ln 2/k$, where the Malthusian parameter k is $\beta\langle Y\rangle(2^{1/(X_{max}+1)} - 1)$, but the average cell generation time is $(X_{max} + 1)/(\beta\langle Y\rangle)$.

(iii) The average, variance and higher moments of the daughter cell distribution of generation times [from equation (28)] are not the same as the average, variance and higher moments of the mother cell distribution of generation times [from equation (26)]. This is because the distribution in the daughter cells' initial number of fibrillar centers is different from the distribution of fibrillar centers among the mother cells at the time of their formation. In other words,

$$\sum_{y_0=0}^{Y_{max}} f(\cdot, y_0; \infty)\Pi(y_0 \to y) \neq f(\cdot, y; \infty). \tag{29}$$

Using the nomenclature introduced by Powell [176], we will call $f(\cdot, y; \infty)$ the "real" distribution of Y and define $F(y)$ as the "artificial" distribution that satisfies the equation

$$\sum_{y_0=0}^{Y_{max}} F(y_o)\Pi(y_0 \to y) = F(y). \tag{30}$$

$F(y)$ may be found by making an initial guess, say $f(\cdot, y; \infty)$, and then iteratively multiplying the result by $\Pi(y_o \to y)$ until convergence is obtained. To the extent that $F(y)$ and $f(\cdot, y; \infty)$ are nearly identical, the distribution of mother and daughter generation times will be nearly the same. If that is the case, we may then use pooled time-lapse microcinematography data to estimate the parameters of the forward distribution that is defined in equation (26). An example is the data considered in Figs 5–7. The average generation times for

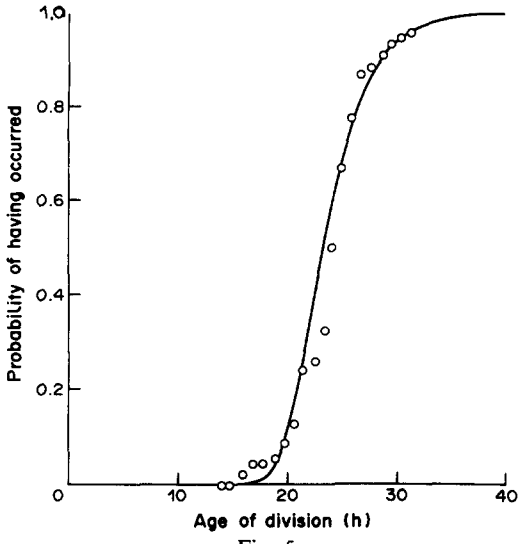

Fig. 5

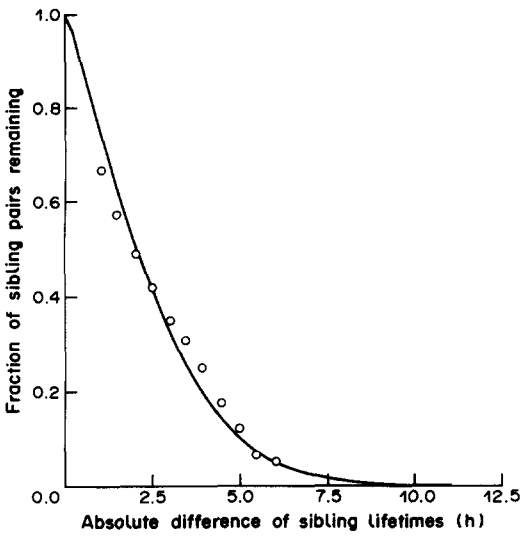

Fig. 6

Fig. 5. Distribution of intermitotic times. The open circles represent the fraction of rat hepatoma cells that have divided by the indicated age, measured by time-lapse microcinematography [47, Fig. 2]. The observed distribution was fitted by the inherited rate model [equation (26)] with parameters $X_{max} = 150$, $Y_{max} = 10$, $\beta = 1.3 \times 10^{-2}$, $\lambda = 1.3 \times 10^{-4}$ and $\mu = 2.6 \times 10^{-5}$. For these values, the model correctly predicts the observed correlations between the intermitotic times of mother–daughter and sibling cell pairs (0.55 and 0.7, respectively; see Fig. 7) as well as the data shown in Fig. 6. The average number of fibrillar centers is predicted to be 0.86 Y_{max}, with a coefficient of variation of 0.11.

Fig. 6. Distribution of the differences between sibling cell generation times (β curve), observed in the experiment illustrate by Fig. 5. The calculation was made using equation (27). The parameters used to simulate the β curve are the same as those indicated in the legend to Fig. 5.

mother and daughter cells were estimated to be 1.0422 and 1.0497 population doubling times, respectively, and the coefficients of variation for the two distributions were 0.158 and 0.161, respectively. This small difference is comparable to what we may expect to arise due to technical factors in time-lapse microcinematography experiments (depletion of nutrients during long-term filming, cell crowding, selection of film interval etc.), so the "real" and "artificial" distributions are practically the same. A similar conclusion was reached by Staudte and Cowan [178] through analysis of a different model.

Figures 5 and 8 illustrate the model's ability to fit observed distributions of cell generation times. Corresponding curves for the distribution of the absolute difference between sibling cell generation times (β curves) are provided in Figs 6 and 9, respectively. In both examples, the sibling cell generation times were observed to show strong, positive correlations, 0.70 and 0.63, respectively. However, the mother–daughter correlations were quite different in the two experiments. For the experiment whose data are shown in Figs 5 and 6, the mother–daughter correlation was observed to be 0.55. In the experiment shown in Figs 8 and 9, a numerical value for the mother–daughter correlation was not reported, but the authors said that they checked to see that "there was no significant correlation between parent and progeny generation times" [42]. Figures 7 and 10 demonstrate how it is possible for the mother–daughter correlations to be so different, even though the sibling correlations have comparable values. Both the sibling and mother–daughter correlations rise and fall as the model's parameters are varied, but the latter is always less than the former, peaks earlier than the former and goes to zero faster than the former. Therefore, a relatively small change in the model's parameters may cause an abrupt drop in the mother–daughter correlation, with only a modest change in the sibling correlation. Finally, note from Fig. 9 that the absolute difference between sibling generation times may have an apparently exponential distribution, even though the number of random cell cycle transitions is much greater than unity [35, 51]. Refer to Brooks *et al.* [42, Fig. 4A] to compare the fit in Fig. 9 with the one obtained using a true exponential.

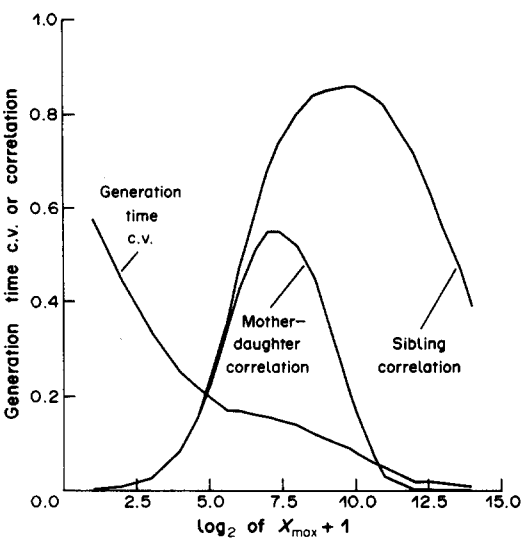

Fig. 7

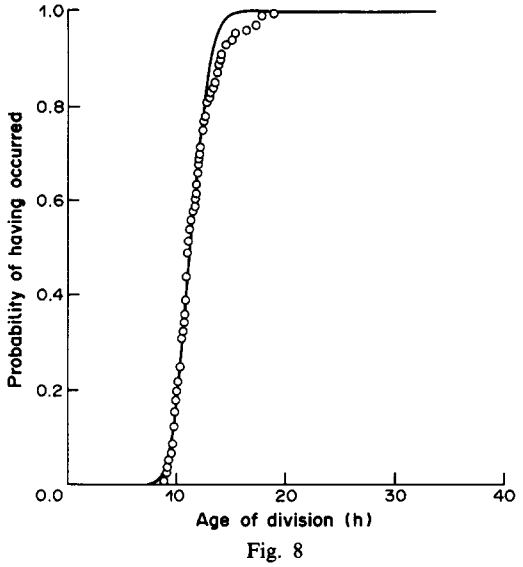

Fig. 8

Fig. 7. Correlations between the intermitotic times of mother–daughter and sibling cell pairs, as a function of the model's parameters. This figure illustrates predictions of the inherited rate model: that the mother–daughter correlations will be less than the sibling correlations, and the latter may in fact be nearly zero while the former are still large. The parameters are the same as in Fig. 5, except that X_{max} is varied over a wide range. The shapes of the curves would be the same if other combinations of parameter values were used, but the location and heights of the peaks would change (see Fig. 10). Behavior of the coefficient of variation of the cells' intermitotic times is also representative: it decreases as X_{max} is increased, with an inflection whose location and width is a function of the parameter values. These moments were calculated by averaging the joint distribution given by equation (28).

Fig. 8. Distribution of intermitotic times. The open circles represent the fraction of 3T3 cells that have divided by the indicated age, measured by time-lapse microcinematography [42, Fig. 4A]. The observed distribution was fitted by the inherited rate model [equation (26)] with parameters $X_{max} = 155$, $Y_{max} = 10$, $\beta = 2.5 \times 10^{-3}$, $\lambda = 1.0 \times 10^{-4}$ and $\mu = 1.4 \times 10^{-4}$. For these values, the model predicts the observed correlations between the intermitotic times of mother–daughter and sibling cell pairs to be 0.03 and 0.61, respectively (see Fig. 10). The average number of fibrillar centers is predicted to be 0.43 Y_{max}, with a coefficient of variation of 0.36.

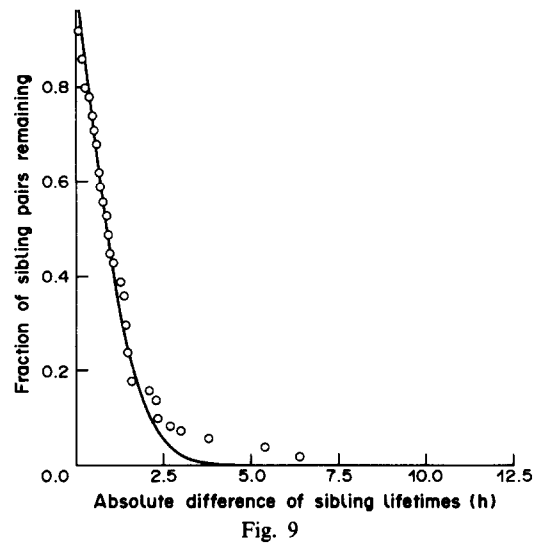

Fig. 9

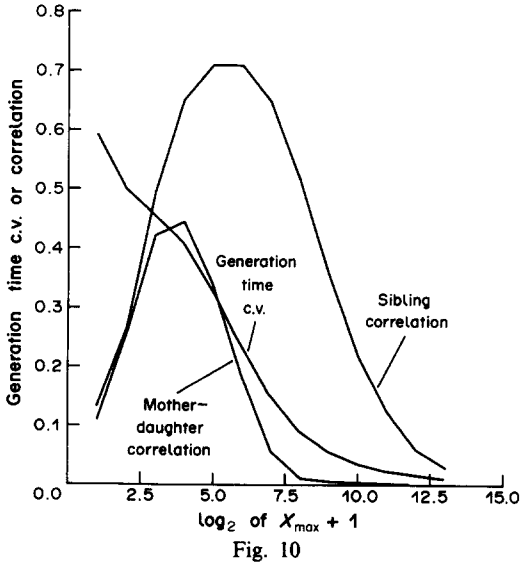

Fig. 10

Fig. 9. Distribution of the difference between sibling cell generation times, observed in the experiment illustrated by Fig. 8. The parameters used to simulate this β curve are the same as those indicated in the legend to Fig. 8. This curve is nearly exponential. For comparison with a fit using an exactly exponential distribution see Ref. [42, Fig. 4A], and note that the last few data points are not fitted by an exponential curve.

Fig. 10. Correlations between the intermitotic times of mother–daughter and sibling cell pairs, as a function of the model's parameters. The parameters used to generate these curves were the same as those in Fig. 8, except that X_{max} was varied over a wide range. Refer to the legend of Fig. 7 for more information.

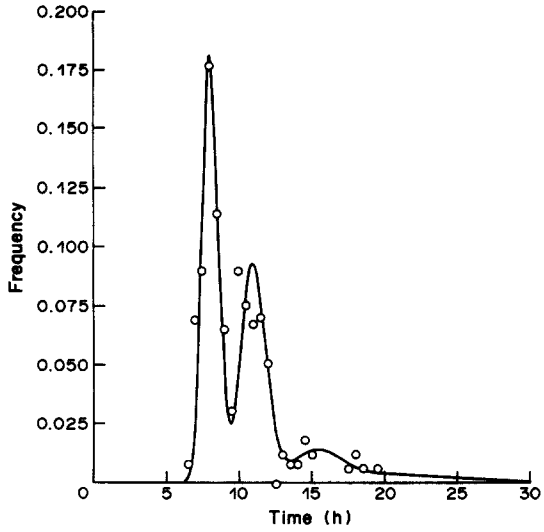

Fig. 11. Quantization of intermitotic times. In some time-lapse microcinematography experiments, the distribution of cell generation times is observed not to be uni-modal. The data here are from Klevecz and Shymko [180]. The inherited rate model explains these data as the result of two factors: (i) the potential number of independent transcriptional centers (Y_{max}) is small, so the mixture of cell types will be noticeable; and (ii) the distribution of cell types at the start of the experiment is somewhat different than what would be observed in the "steady state", i.e. $f(\cdot, y; \infty)$. Parameters used to fit the data were $X_{max} = 163$, $Y_{max} = 3$, $\beta = 7.0$, $\lambda = 0.07$ and $\mu = 0.004$, with initial conditions $f(\cdot, 1) = 0.1$, $f(\cdot, 2) = 0.4$ and $f(\cdot, 3) = 0.5$.

The inherited rate model predicts that for an exponentially growing population, the shape of the distribution of generation times will resemble a gamma distribution: unimodal with a tail to the right. This may seem surprising since the distribution defined by equation (26) is a mixture of distributions. However, the mixing is not apparent since the weighting vector, $f(\cdot, y; \infty)$, is precisely what is required to generate unimodality. If the cells are not in the "steady state" of exponential growth (as discussed in the next two sections), the weighting vector is dependent on the detailed prior history of the cell population and may be such that the mixing of cell types generates a multimodal compounded distribution. Figure 11 gives an example of a distribution that is not unimodal, previously attributed to the periodicity of a chemical clock [179, 180]. The suggestion here is that the series of preferred generation times is a reflection of the discrete number of potential independent transcriptional centers in the cell.

7. TIME-DEPENDENT BEHAVIOR OF THE POPULATION

A. Near "Steady State" Populations; Population Entropy

Populations that are not growing exponentially often arise through the selection of sub-populations within the "steady state" population. An example that is treated below is the fraction-labeled-mitoses experiment, in which S phase cells are selected by labeling at an initial time point. This subpopulation grows quasi-synchronously until its members redistribute themselves among all of the cell cycle phases, eventually satisfying equation (9). In principle, the evolution of the population from an arbitrary initial condition may be calculated analytically by using linear transform methods to solve equations (2a, b). As a practical matter, it is easiest to numerically integrate the differential equations (6a–c) or (14a, b), unless the perturbation from exponential growth is slight. In that case, the non-linear terms in equations (14a, b) are negligible, and they become a set of linear differential equations that may be solved by linear transform methods. The procedure is discussed in Appendix D. The analysis there provides characteristic damping and frequency constants as functions of the model's parameters. The analysis also explains why the perturbed population will return asymptotically to the "steady state" of exponential growth: the

"steady state" given by equation (9) is asymptotically stable as defined in the qualitative theory of differential equations [181, p. 155]. That being the case, it is possible to construct a function of the state of the perturbed population having the following property. This (Lyapunov) function always increases as time progresses, reaching a constant value when the population eventually grows exponentially. The increase in value will be observed whether perturbation of the population is small or large. In thermodynamic nomenclature, this function is an entropy. It may be used as a measure of the disorder of the population and as a measure of the extent to which a population deviates from its "steady state" properties (Fig. 13).

B. Fraction-labeled-mitoses (FLM) Curves

Assume that a cell is in the G1 phase if its X value is between 0 and X_{G1S}, that an S phase cell has a value of X between $X_{G1S}+1$ and X_{SG2}, that a cell in the G2 phase has a value between $X_{SG2}+1$ and X_{G2M}, and that a mitotic cell has an X value between $X_{G2M}+1$ and X_{max}. When the S phase cells of an exponentially growing population are labeled with radioactive thymidine [182, 183], we are then dealing with two populations: the labeled population, which initially is not in the "steady state", and the original population (labeled + unlabeled), which is assumed to continue its exponential growth.

Let $\Delta f(x, y; t)$ denote the deviation of the labeled cells from the "steady state" fractions. Define the time of (instantaneous) labeling to be $t = 0$, and let

$$\begin{aligned} &\Delta f(x, y; 0) = 0 && \text{if} \quad X_{G1S}+1 \leqslant x \leqslant X_{SG2} \\ &\Delta f(x, y; 0) = -f(x, y; \infty) && \text{otherwise.} \end{aligned} \tag{31}$$

The fraction of cells that are labeled, among unlabeled + labeled cells in the indicated (x, y) state, is given by

$$\mathrm{FL}(x, y; t) = \left[1 + \frac{\Delta f(x, y; t)}{f(x, y; \infty)}\right] \exp\left[\sum_{y=0}^{Y_{max}} \beta y \int_0^t \mathrm{d}t' \Delta f(X_{max}, y; t')\right], \tag{32}$$

where $\Delta f(x, y; t)$ satisfies equations (14a, b), given the initial conditions specified in equations (31). Then, the fraction of labeled mitotic (FLM) cells is

$$\mathrm{FLM}(t) = \frac{\sum_{x=X_{G2M}+1}^{X_{max}} \sum_{y=0}^{Y_{max}} f(x, y; \infty)\mathrm{FL}(x, y; t)}{\sum_{x=X_{G2M}+1}^{X_{max}} \sum_{y=0}^{Y_{max}} f(x, y; \infty)}. \tag{33}$$

By varying the parameters of the inherited rate model (including the location of the cell cycle phases in the range 0–X_{max}), it is possible to fit observed FLM data. In so doing, one obtains estimates for the distribution in the duration of the cell cycle phases. Figure 12 illustrates fitting of "textbook" FLM data, in which the oscillations persist for a few generations, with a gradual damping. Many models may be used to fit data that are so regular [184]. In fact, the gamma function model [see equations (24a, b)] works well for these data, so they may be used to illustrate the increase in entropy that is predicted by equation (D.9), shown in Fig. 13.

The usefulness of the inherited rate model is more apparent when the data do not conform to the ideal. This is because the three parameters β, λ and μ allow greater control over simulation of the damping characteristics of the population than is possible with simpler models. Steel [182, Chap. 4] discusses circumstances in which conventional models are unable to fit the observed FLM data. The inherited rate model is able to explain some of these data, as shown in Fig. 14. A further illustration of the model's flexibility is shown in Fig. 15. It shows two simulated FLM curves having virtually identical initial portions, but having quite dissimilar terminal segments.

An additional example is provided in Fig. 16. It is not an FLM curve but illustrates the same phenomenon, the decay of synchrony of a cell population. Fit of the data by the inherited rate model is better than that obtained if correlations are not allowed and is comparable with the fit obtained by Rubinow's [52] model. The fit is not as good as with the model of Voit and Dick [185], but the latter model required 30 parameters and 5 initial conditions, as compared with 5 parameters and calculated initial conditions for the inherited rate model.

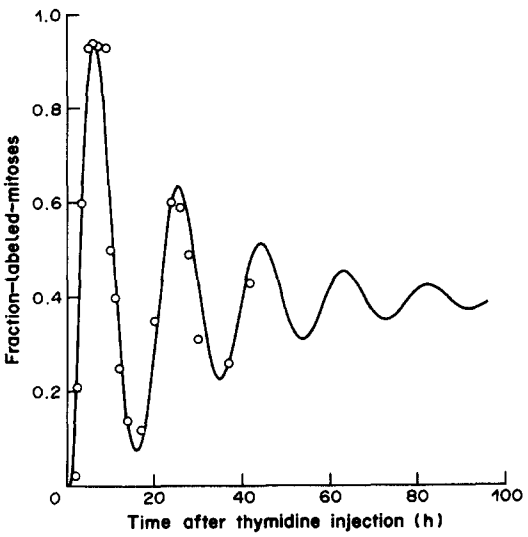

Fig. 12

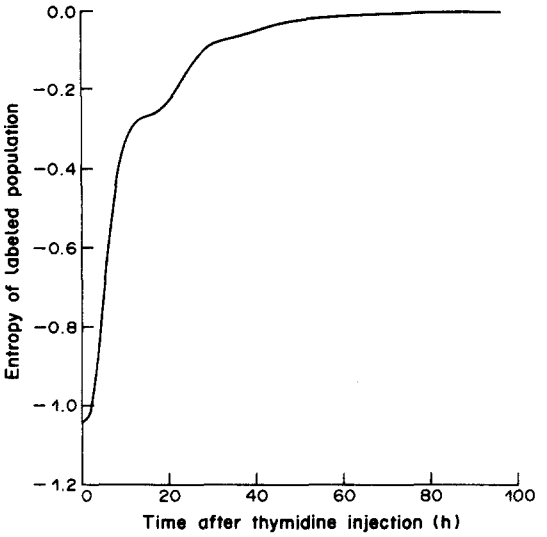

Fig. 13

Fig. 12. Ideal fraction-labeled-mitoses curve. When the fraction of labeled mitoses [equation (33)] show smooth, damped oscillations, as in these data from Hartman *et al.* [184, Fig. 1C], the gamma function model may be used as a limiting case of the inherited rate model. The parameters used to fit the data were $X_{G1S} = 11$, $X_{SG2} = 23$, $X_{G2M} = 26$, $X_{max} = 27$ and $\beta\langle Y\rangle = 0.69$.

Fig. 13. Entropy of a cell population. If a cell population is initially out of the "steady state", its entropy [equation (D.9)] will increase until the "steady state" is achieved. This figure describes a population of cells that were initially all in the S phase (the labeled cells in the experiment presented in Fig. 12). Maximum entropy is achieved when the cells redistribute themselves among all the cell cycle phases. Parameters values are as indicated in the legend to Fig. 12.

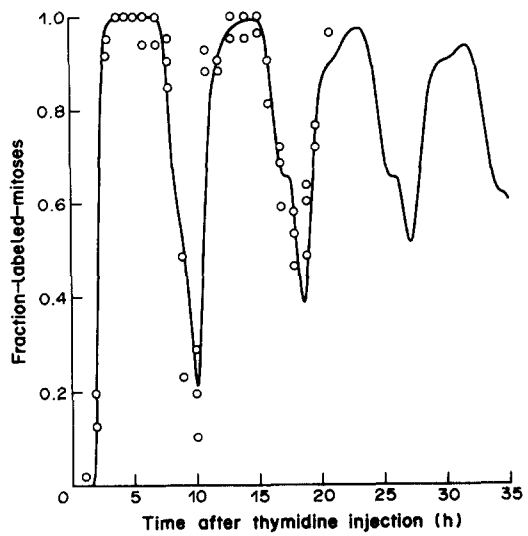

Fig. 14

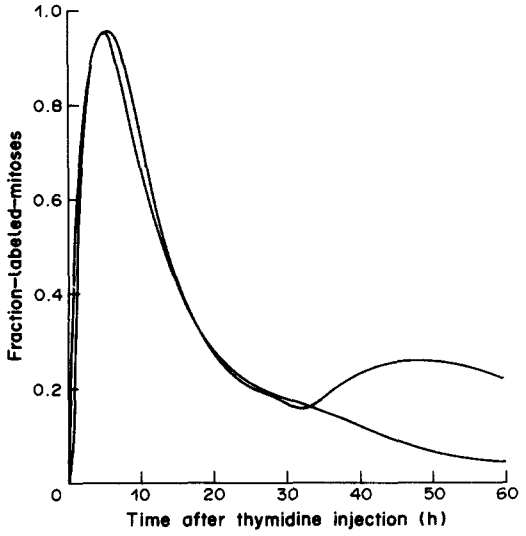

Fig. 15

Fig. 14. Ability of the inherited rate model to fit fraction-labeled-mitoses data that are difficult to fit by other models. These data were selected by Steel [182, Fig. 4.7F] as an example of some that are difficult to fit by conventional models. The inherited rate model is able to reproduce the sharp rise and fall of the oscillations, as well as the rise in the successive minima. According to the model, these features are due to the heterogeneous rates of cell proliferation. Mixing of the different cell types is apparent in the later oscillations. Parameters for the simulation were $X_{max} = 75$, $Y_{max} = 10$, $\beta = 0.89$, $\lambda = 4.4 \times 10^{-3}$, $\mu = 4.4 \times 10^{-4}$, $X_{G1S} = 1$ and $X_{SG2} = 55$.

Fig. 15. Flexibility of the inherited rate model in simulating different damping characteristics of fraction-labeled-mitoses curves. Two curves are shown, both of which have nearly identical initial segments, but which separate abruptly around 30 h. The flexibility that is demonstrated here is due to the model's representation of the population as a mixture of subpopulations. Parameters for the two curves were $X_{max} = 75$, $\beta = 0.3$, $\lambda = 1.4 \times 10^{-2}$, $\mu = 1.4 \times 10^{-2}$, $X_{G1S} = 60$, $X_{SG2} = 72$; $X_{max} = 63$, $\beta = 0.08$, $\lambda = 1.7 \times 10^{-4}$, $\mu = 2.9 \times 10^{-4}$, $X_{G1S} = 55$ and $X_{SG2} = 62$. In both cases, $Y_{max} = 10$ and $X_{G2M} = X_{max} - 1$.

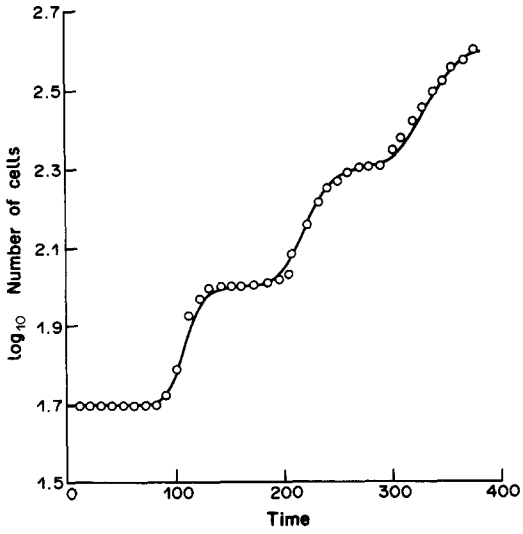

Fig. 16. Decay of synchrony of an initially synchronous cell population. These data were used by Rubinow [52] and by Voit and Dick [185] to demonstrate the superiority of their models over simple stage models that do not allow for correlations between the intermitotic times of mother and daughter cells. The inherited rate model [equations (2a, b) and (3)] also permits a somewhat better fit than a simple stage (gamma function) model, due to its ability to accommodate different damping characteristics of population growth.

8. POPULATION GROWTH IN THE PRESENCE OF CYTOTOXIC AGENTS

A. Limiting Tissue, Resistant Cells, Doses and Fractionation Schedules

The failure of treatment in a large percentage of cancer patients is due to two problems. One is the lack of specificity of the cytotoxic agent for the tumor cells: it is not possible to destroy the tumor without at the same time inflicting massive—and potentially life-threatening—damage to normal tissue. The damaged normal tissue is usually either the hemopoetic system or the gut epithelium, and is called the limiting tissue for a given therapeutic protocol. The second problem is the existence of resistant cells within the tumor. Increasing the dose of the cytotoxic agent may circumvent the latter problem [186], but this necessarily aggravates the former problem.

The effectiveness of chemotherapeutic agents often depends on the dose and schedule of administration. This has been demonstrated in numerous toxicity studies involving rodent models [187]. There almost certainly exist optimal dose-schedule protocols for humans as well, but it is not possible to try all the possibilities in patients, for obvious ethical reasons. If primate models were used, it might be possible to extrapolate toxicity results to the clinic, but this is also prohibitive for practical reasons. As a result, protocols that are now in use are found empirically, with no guarantee that they are optimal.

The possibility of using cell kinetic models to predict the optimal fractionation schedule has been discussed by several investigators [188–191]. However, models that have been proposed for this purpose are not complete enough to satisfy the needs of the clinician [182, 192]. Deficiencies of models of chemotherapy include their oversimplification of pharmacokinetic factors, their omission of the effect of circadian rhythms [193, 194] and their inability to represent heterogeneity of the cells' response to chemotherapeutic agents. Similar models that have been proposed for use in therapeutic radiology give only a simplified account of the additional complicating factors that arise there, namely, the reoxygenation and repair of irradiated tissue [195, 196]. Nevertheless, these models have been used to recommend one or another strategy in the design of protocols, even if they have not yet been successful in recommending particular doses and fractionation schedules.

The purpose of what follows is not to propose a complete model of therapeutic protocols, but rather to model one aspect of the problem for which no satisfactory account has been given: the heterogeneity of cellular response to cytotoxic agents and the kinetics of tumor relapse. The rationale for the simulations described presently is that rapidly growing cells are thought to be

easier to kill than slowly growing cells. In the context of the inherited rate model, the postulate is that among the cells of the population, those whose rDNA genes are being actively transcribed are at greatest risk of damage by the agents. This is not to say that the actively transcribed rDNA genes are necessarily the target of the cytotoxic agent, only that there is a correlation due to any of several factors. For cycle specific drugs, the cells at greatest risk could be the ones that are most metabolically active and which would transport the cytotoxic drugs at the greatest rate; they could proceed through the cell cycle fastest so as to freeze damage faster than it could be repaired; and/or they could be producing products in addition to rRNA at an elevated rate, some of which are needed for conversions of the agent to its active form. For phase specific drugs, resistance of the slowly growing cells would be attributable to the failure of many of these cells to be present in the susceptible cell cycle phase during short-term therapy.

B. Simulation of Population Growth in the Presence of Cytotoxic Agents

Single-dose–survival curves

A review of the growth and survival of stem cells in the presence of cytotoxic agents is provided by Steel [182, Chap. 7]. The first point to be made is that the survival curves shown by Steel may be interpreted with the aid of the inherited rate model: a population is intrinsically heterogeneous with respect to its cells' survival in the presence of some chemotherapeutic agents, and the inherited rate model may be used to generate a distribution for this heterogeneity. The example that we consider is the response to the drug Ara-C [182, Fig. 7.12f; 197]. This is one of the most commonly used drugs for leukemia, an anti-metabolite that interferes with DNA polymerase and that is incorporated into DNA and RNA, producing defective macromolecules. Although it is often considered to be an S phase specific agent (because DNA synthesis is inhibited by virtue of its effect on DNA polymerase), the data show that the situation is more complicated. As shown in Fig. 17, 90% of the (L1210 leukemia) stem cells are rendered non-clonogenic within 15 min of exposure to a single low dose of Ara-C. At single high doses, resistance by roughly 1% of the population is apparent. Consider the form of the dose–survival curve. If there were two subpopulations, sensitive and insensitive, and if the likelihood of non-clonogenicity of a sensitive cell falls as $\exp(-D/D_{37})$, where D is the dose, then there will be a steep drop in clonogenicity with increasing dose, followed abruptly by a plateau (lower curve, Fig. 17). This is clearly not the case. A better fit is obtained if we assume that the dose–survival curve is of the form

$$\frac{N(D)}{N_0} = \sum_{y=0}^{y_{\max}} f(\cdot, y; \infty) \exp[-D/D_{37}(y)] \tag{34}$$

where the rate constant $D_{37}(y)$ is inversely proportional to y, above some threshold of y. That is to say, cells whose number of fibrillar centers is less than some threshold value are producing rRNA at a rate so low that the Ara-C incorporated into their RNA is insufficient to render them non-clonogenic ($D_{37} = \infty$). They are therefore considered to be resistant. Above this threshold, incorporation of the Ara-C increases in proportion to the number of fibrillar centers present in the cell, accounting for the gradual drop in survival at high doses (cells with low value of y) and for the steep drop in survival at low doses (cells with high value of y). Thus, the likelihood of cell death is taken to be proportional to the amount of Ara-C that is incorporated into RNA, which has been observed experimentally [198, 199]. Usefulness of the inherited rate model is in providing an $f(\cdot, y; \infty)$ with which to represent the heterogeneity of the population's response to Ara-C.

Multiple-dose–survival curves

Chemotherapeutic protocols often involve the periodic administration of one or more cytotoxic agents. Such protocols may be simulated using equations (7a, b), assuming that a certain fraction of the population's stem cells are rendered non-clonogenic at each exposure to the drug. Growth of the population will be more complicated than that predicted with simpler models since the distribution in fibrillar centers (y) is assumed to change with each episode of drug administration, i.e. cells with large values of y are preferentially killed, resulting in a non-"steady state" distribution (that will eventually reachieve its "steady state" form if the population were subsequently allowed

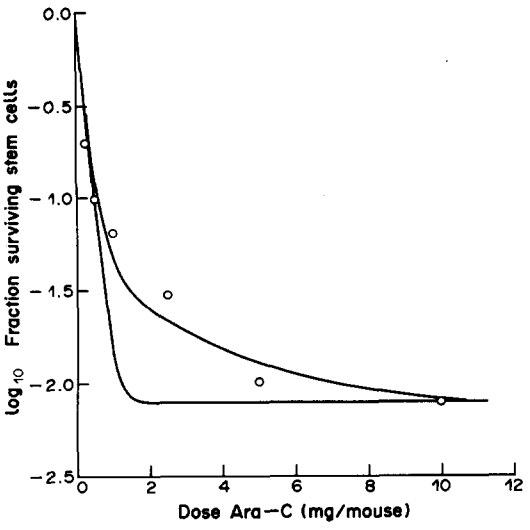

Fig. 17

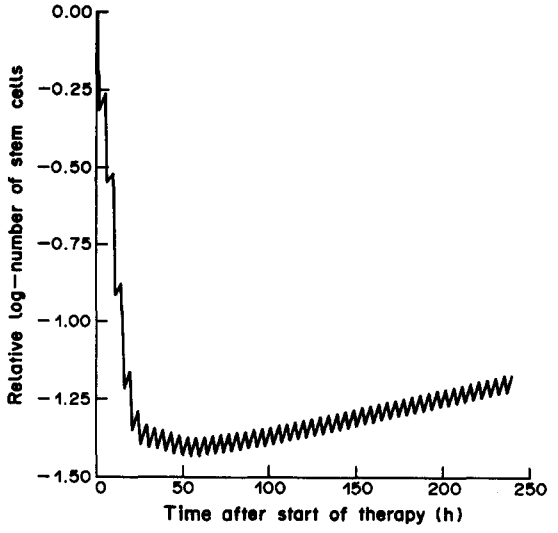

Fig. 18

Fig. 17. Heterogeneity of cellular response to a single dose of cytotoxic agent. Here, 1% of L1210 leukemia cells are shown here to be resistant to the anti-metabolite Ara-C [182, Fig. 7.12f]. If there were only two subpopulations, resitant and susceptible, survival as a function of dose would be as in the lower curve. A better fit is obtained if we assume that there are several subpopulations, each having a different response to the drug. The inherited rate model may be used to generate the fraction represented by each subpopulation (upper curve).

Fig. 18. Survival of stem cells after multiple, periodically administered doses of a cytotoxic agent. Growth of the population is described by the inherited rate model [equations (7a, b)]. Every 5 h, cells are killed by the drug, with preferential loss of those having many fibrillar centers (large Y, rapidly growing cells). Resistant cells (those with low Y values) continue to proliferate, causing the population to eventually relapse to its original size. Asymptotic exponential growth by the envelope of the number of cells is discussed in Appendix D.

to proliferate without interference). To simulate an actual protocol, both the tumor and normal limiting tissue would have to be modelled under a variety of possible dose-schedule choices, but this is beyond the scope of the present discussion. Rather, the general kinetic characteristics that will be observed for each simulation, shown in Fig. 18, are pointed out. The population growth will be observed to show three phases. During the first phase, there is a rapid decrease in the size of the stem cell population. During the second phase, the population size stabilizes to a plateau level. During the final phase, there is a gradual regrowth (relapse) of the population to its original size. This regrowth is due to the resistant cells, whose number of fibrillar centers lies below the threshold of sensitivity (Fig. 17). The details of the growth kinetics are clearly a function of many factors: the kinetic characteristics of the particular tumor or limiting normal cell type (X_{max}, Y_{max}, β, λ and μ), the frequency and dose of the administered agent, whether the agent is phase specific or not, and the threshold y value, below which cells are considered to be resistant to the drug. In the optimal protocol, we wish the plateau phase to be extended and lowered considerably for the tumor cells and to be abbreviated and heightened for the normal cells. In fact, in the ideal protocol, the size of the tumor stem cell population would be decreased to a size that is so small that the deterministic model is no longer appropriate. Survival curves comparable to the simulation shown here are given by Steel [182, Fig. 7.13]. In agreement with the simulation shown here, these experimental curves are observed to exhibit more than one phase, which may be interpreted to reflect an initial loss of sensitive stem cells, followed by kinetics of the insensitive stem cells. Note that the envelope of the log-number of stem cells in Fig. 18 grows linearly after the cells enter the phase of relapse. This asymptotic behavior of a periodically perturbed population is not unexpected. The cyclic variation of the population between episodes of cytotoxicity, plus exponential growth (or decline) of the population over the long term, is reminiscent of population growth in the presence of circadian rhythms. Theorems that explain this asymptotic growth of a periodically perturbed population are discussed in Appendix D.

9. DISCUSSION

A. Summary of the Model's Properties

The inherited rate model of the cell cycle combines features of several previously described models. It makes use of the stage concept, which was introduced by Kendall [170] and has been used by many subsequent investigators [171, 172, 190, 200–202]. It emphasizes the rate of cell cycle progression, as in the models of Sisken and Morasca [50] and Castor [51]. It is compatible with the possibility that the number of cell cycle stages may be large, but that the cell cycle duration remains random, which is a distinguishing feature of maturity models [52–55]. It is also a "physiological" model in the sense that it assigns a role to a particular cell property (nucleoli), as has been done in models that describe centriole events [42], cell size [25–27, 38, 39], RNA and protein content [29], initiator and inhibitor protein levels [179, 203] etc. Not surprisingly, then, several properties of the inherited rate model are to be found among these previous models. The properties that recommend its use for the understanding of cell kinetic phenomena are as follows:

(i) The model is concrete as to the physical meaning of the variables involved. If a cell's state were described by only a single variable representing cell cycle maturity, it would not be so important to be specific about the variable's meaning. Hopper and Brockwell [204, 205] express the attitude as follows: "It is tempting to ascribe some biological significance to the maturity, e.g. to suppose that each increase in maturity corresponds to completion of some well-defined biochemical stage in the development of a cell. We do not, however, claim any such significance. For us, the introduction of maturity is simply a convenient mathematical device for setting up a standard cell kinetic model." But when the cell's state is specified by two or more variables in order to explain how a cell's inheritance predisposes it to divide at a particular age, it is difficult to propose a credible model for how the inherited variable influences the maturity variable without providing experimental evidence that the variables are in fact physically meaningful. In the inherited rate model, the nucleolar variable may be visualized in mitotic cells so as to justify the way that inheritance is treated, and the mechanism relating cell cycle progress to the nucleolar variable is that both are controlled by components of the ubiquitin system, which in turn is closely related to the mechanism of protein turnover and its control by growth factors.

(ii) The inherited rate model *predicts* the initial conditions, i.e. $f(\cdot, y; \infty)$, in an exponentially growing population, for given parameter values. Similarly, the form of the distribution of generation times is *predicted* by the model to be a consequence of the postulated mechanism, rather than being postulated *a priori*. The latter approach is regarded by detractors as an exercise in curve fitting [49].

(iii) The model accounts for the observation of positive correlations between the generation times of sibling and mother–daughter pairs, explains why the latter correlations will be smaller than the former, and includes the possibility that the mother–daughter correlations may be nearly zero as a special case, even if the sibling correlation is large. Its explanation for the correlations is as follows: (1) newly-formed sibling cells are more like one another than randomly selected pairs of cells; (2) the inherited state of a cell predisposes that cell to divide at a particular age; (3) the inherited state of a cell tends to persist as the cell ages. When factor (3) is relatively insignificant, a cell will have no memory of its initial state by the time that it divides, and the mother–daughter correlation will be small. If that is the case, factors (1) and (2) may nevertheless be sufficient to cause the sibling correlations to be significant. By the same reasoning, the model predicts that there will be a correlation between the times that sibling cells spend in a particular phase of the cell cycle and that the G1 phase correlation will be greater than that of the later phase durations. Further corollaries are that the duration of phases in each cell will be correlated, and the correlation between the G1 and S phase transit times will be greater than the correlation between the duration of G1 and G2 (or M). The model

also provides for an approximately exponentially distributed absolute difference between sibling generation times as a special case of parameter values and provides justification for the common practice of pooling intermitotic times from different generations in time-lapse microcinematography experiments. It explains the observation of preferred (quantized) generation times as a consequence of the fact that the population is a mixture of cells having different inherited rates of cell cycle progress.

(iv) The model contains few parameters. It is sufficiently simple that many of its properties may be calculated analytically. The importance of analytical tractability cannot be over-emphasized since this property makes practical the variation of parameter values so as to fit observed data. The model is mathematically interesting in its own right as an example of the problem of mixing probability distributions in such a way as to achieve a particular compounded distribution.

(v) Development of the model focuses on the *fraction* of cell in each cell cycle state, rather than the *number* of cells. This is useful for two reasons. First, it introduces the stability theory of differential equations into the analysis, explaining why the exponential growth of the population is asymptotically stable, allowing the calculation of damping and oscillation parameters and allowing us to define an entropy for the population. The second advantage is practical. When calculating fraction-labeled-mitoses curves (for example), integration of the rate equations for cell numbers [equations (2a, b)] leads to large numbers and numerical errors, in contrast to integration of the rate equations for the fractions [equations (6a–c) and (14a, b)]. The disadvantage of performing the analysis by referring to the fractions is that the rate equations become non-linear [equations (6a–c)]. However, the non-linearity is benign for the same reason that a Riccati equation is manageable: the non-linear equations may be transformed back into linear equations if necessary. A consequence of this linearity is that the time derivatives of the first moments are functions only of the first moments [equation (3)]. If the transitions in equations (1a–d) were non-linear functions of the random variables, the differential equations in equation (3) would contain terms involving the variances and covariances of the $N(x, y)$, and a hierarchy of moment equations would have to be considered. See Appendix A.

(vi) The model may be used to analyze the three types of experiments mentioned in Section 3B. This is because the model was formulated in terms of mechanisms and transitions [equations (1a–d), rather than simply as a postulated distribution with unknown parameters. The price to be paid for the model's versatility is that distributions had to be calculated (Sections 4–6) before data could be fitted to them. Examples of data fitting were given for the distribution of cell generation times, fraction-labeled-mitoses curves and decay of synchrony curves. Fitting of data describing the distribution of cell cycle states and of the number of fibrillar centers was not attempted here for the following reason. To analyze these data, it is necessary to present an auxiliary model for the experimental procedure itself. The situation is analogous to the analysis of flow cytometric data, in which the problem is not simply to understand the relation between the distribution of DNA content and the fraction of cells in each cell cycle states, but also to extract the distribution of DNA content from the data. This requires considerable discussion and analysis [23, 24]. Similarly, analysis of premature chromosome condensation data requires a model for artifacts that arise during cell fusion procedures, and the analysis of silver staining requires a model for the way that deposits form under a particular staining protocol. Models for these data will be provided in a subsequent paper.

(vii) Many models of cell proliferation assign "proliferating" and "non-proliferating" cells to different compartments. This assignment is one of convenience and does not allow for the possibility that there is a spectrum of cell types that differ with regard to their rates of proliferation. The inherited rate model may be more realistic in that it allows for Y_{max} rather than two cell types. This feature is useful in modelling the heterogeneous response of cells to cytotoxic agents, provided that lack of response

to these agents is also a distributed property and is correlated with the heterogeneity of cell growth rate [206].

(viii) The most physically realistic representation of the cell cycle is as a random process. Although the inherited rate model describes the cell by such a process, some events that underly the randomness could conceivably be deterministic [12] in the same way that a pseudo-random number generator is deterministic—differential equations describing the cell's chemistry are non-linear by virtue of the feedback inherent in the presence of control mechanisms. Under certain circumstances, such differential equations exhibit chaotic (pseudo-random) behavior [207]. True stochastic fluctuations will exist in addition to any deterministic chaos, since they are present in all chemical reactions [167, 168] and in systems involving the diffusion of metabolites [208, 209]. The fluctuations will be pronounced in a cell because macromolecules with essential functions may be present at a level of a few molecules per cell [13, 34, 58]. In fact, fluctuations in the activity of individual macromolecules, sometimes of known location within individual living cells, have been measured [210–213].

Given that a stochastic model is appropriate, comment should be made concerning the form of the model that was adopted here: a bivariate Markov process with a finite number of states. A more general model might have been constructed by allowing the random waiting time in each state to have a distribution other than exponential [e.g. 214]. I would argue, through, that the use of a non-Markov distribution of waiting times is simply a device to hide variables that have been omitted from the more complete Markov process (e.g. use of a semi-Markov process with a few variables to represent a true Markov process with many variables). Additional variables are already implicitly hidden in the parameters of the model: just as the expected value of Y is hidden in the parameter of a one-variable stage model [see the comments after equations (24a, b)], so too the parameters in equations (1a–d) hide additional variables related to the transitions that they characterize. A subtle concealment of variables is also implicit in the adoption of a model in which X is an integer random variable ranging from 0 to X_{max}. A criticism of integer stage models has been that cell cycle maturation is a continuous process, and the only reason for making X_{max} finite is that when X_{max} is large enough to approximate continuity, the indeterminacy required of the model disappears [170]. The addition of one or more random variables (e.g. Y) to the simple stage model relieves X of the burden of carrying all the cell's indeterminacy and, as a consequence, X_{max} may assume a larger value in order to achieve a particular coefficient of variation of intermitotic times. In fact, if Y_{max} did not represent the necessarily finite number of rDNA genes in the cell, we could make Y_{max} arbitrarily large, so that X may approximate the (continuous, random) integral of a white noise process.

B. Extensions of the Model

Many extensions of the model are possible, most of which would involve the addition of parameters. Several that come to mind allow: the reversibility of cell cycle progress; the rate of cell cycle progression per fibrillar center to be different in the various cell cycle phases; the possibility of an extra random transition in the G1 phase; differences to exist between one nucleolar organizer and another; the number of fibrillar centers to double when the rDNA genes are duplicated; the rate of cell cycle progress to be a non-linear function of the number of actively transcribed genes; the parameters β, λ and μ to be functions of additional variables (e.g. growth factor levels); density-dependent growth inhibition in which the parameters are functions of the population density; spontaneous cell death and terminal differentiation; gradual differentiation in which the parameters are functions of the generation number [215]; for circadian rhythms (see Appendix D); the parameters to be a function of the cell's location within tissue (e.g. the location in the crypt of the gut's epithelium [183]); and random or asymmetric partitioning of the fibrillar centers at the time of cell division. The possibility of unequal daughter cells already has a large literature [12, 29, 34, 35, 38, 39, 216–220].

As regards other extensions, it is useful to distinguish between those that are intended to provide

a more complete representation of a cell's physiology and those that provide a better model of the cell's environment. The guide to selecting additional variables to represent a cell's physiology should be that all variables are defined in experimental terms and that they may be measured in individual cells. The model in its present form describes only ribosomal genes because they are the cell's most actively transcribed genes and because their activity may be measured in individual cells with silver staining procedures. The rDNA genes are certainly not the only ones whose activity influences the rate of cell cycle progression, so one would like to add variables corresponding to these other genes. Cytogenetic methods comparable to silver staining exist for quantifying the activity of arbitrary genes. One method is based on the sensitivity of actively transcribed chromosome regions to nucleases [221, 222]. The other method is based on the tendency of actively transcribed genes to be duplicated before inactive genes [69]. That is to say, the timing of DNA replication in individual chromosome bands, measured by the procedure illustrated in Fig. 2, is a measure of the transcriptional competence of the genes that have been mapped to those bands. Examples of genes that might be included in a more complete model of cellular resistance to cytotoxic agents are those that convey resistance through gene amplification. Although the situation is not entirely comparable to the case of ribosomal RNA genes, the number of resistance genes may rise and fall in much the same way that the y variable of the inherited rate model fluctuates along a cell lineage. Addition of such genes to the model would allow greater freedom in representing the spectrum of heterogeneous cell types than is possible with current models that describe the appearance of mutant cells [223, 224].

A more difficult extension of the model would be one that attempts to provide a complete representation of the ecological factors that influence *in vivo* cell proliferation. It is difficult to see how any single model can describe the three-dimensional organization of tissue as it relates to the availability of nutrients and oxygen, the interactions between cells, cell differentiation and pharmacokinetics, in addition to providing a realistic model of the cell cycle. Such a model would contain so many parameters that it would be difficult to test, even if all of the relevant variables were identified. Additional complications arise if the objective of the model is an accurate prediction of a cancer patient's response to a particular therapeutic protocol since growth of the tumor is not necessarily the proximal cause of death of a cancer patient. For example, a tumor of the pericardium may produce fluid that fills the pericardial space, producing pressure on the ventricles, leading to tamponade and heart failure (the proximal cause of death). To make realistic models of survival, then, it is necessary to simulate not only the kinetics of tumor growth, but also all the mechanisms that can cause a tumor (and its treatment) to kill the patient. Perhaps the prudent response to this biological complexity is to adopt a hybrid biomathematical–statistical approach. Statisticians attempt to make survival predictions using models that do not pretend to represent any of the actual physiological interactions [225], using variables that have no direct bearing on the physiology of tumor growth (age and sex of the patient etc.). The suggestion is to move the analysis one step closer to reality by using a simple kinetic model, such as the inherited rate model, but to estimate its parameters with the aid of some convenient statistical model that relates the parameters to whatever clinical data are available.

Acknowledgements—Support was provided by NIH Grant Nos GM30236, CA39949 and CA06927, and by an appropriation from the Commonwealth of Pennsylvania.

REFERENCES

1. I. J. Fidler and I. R. Hart, Biological diversity in metastatic neoplasms: origins and implications. *Science* **217**, 998–1003 (1982).
2. P. C. Nowell, The clonal evolution of tumor cell populations. *Science* **194**, 23–28 (1976).
3. G. Poste, Cellular heterogeneity in malignant neoplasms and the therapy of metastases. *Ann. N.Y. Acad. Sci.* **397**, 34–48 (1982).
4. A. H. Owens, S. Baylin and D. S. Coffey (Eds), *Tumor Cell Heterogeneity: Origins and Implications*. Academic Press, New York (1982).
5. P. Selby, R. N. Buick and I. Tannock, A critical appraisal of the "human tumor stem-cell assay". *New Engl. J. Med.* **308**, 129–133 (1983).
6. J. T. Leith and D. L. Dexter (Eds), *Mammalian Tumor Cell Heterogeneity*. CRC Press, Boca Raton, Fla (1986).

7. D. R. Rigney, Methods for including cell pedigree in models of cell proliferation. In *Proc. 11th IMACS World Congress*, Vol. 3 (Edited by B. Wahlstrom, R. Henriksen and N. P. Sundby), pp. 81–84. Moberg & Helli, Oslo (1985).
8. C. N. Hinshelwood, *The Chemical Kinetics of the Bacterial Cell*. Oxford Univ. Press, London (1946).
9. A. G. Fredrickson, D. Ramkrishna and H. M. Tsuchiya, Statistics and dynamics of procaryotic cell populations. *Maths Biosci.* **1**, 327–374 (1967).
10. N. R. Hartman and I. J. Christensen, Various applications of the continuity equation in the analysis of data measured by flow cytometry. In *Biomathematics and Cell Kinetics* (Edited by M. Rotenberg), pp. 389–401. Elsevier/North-Holland, Amsterdam (1981).
11. S. Zimmerman and R. A. White, Generalizations of a fluid dynamic model for analyzing multiparameter flow cytometric data. In *Biomathematics and Cell Kinetics* (Edited by M. Rotenberg), pp. 403–409. Elsevier/North-Holland, Amsterdam (1981).
12. M. Witten, Modeling cellular systems and aging processes. *Mech. Ageing Dev.* **17**, 53–94 (1981).
13. R. Duncan and E. H. McConkey, How many proteins are there in a typical mammalian cell? *Clin. Chem.* **28**, 749–755 (1982).
14. E. Holtzman, Membrane circulation: an overview. *Meth. Cell Biol.* **23**, 379–397 (1981).
15. M. S. Bretscher, Endocytosis: relation to capping and cell locomotion. *Science* **224**, 681–686 (1984).
16. P. Cautrecasas and T. F. Roth (Eds), *Receptor-mediated Endocytosis*. Chapman & Hall, New York (1984).
17. W. J. Wickner and H. F. Lodish, Multiple mechanisms of protein insertion into and across membranes. *Science* **230**, 400–407 (1985).
18. S. Penman, A. Fulton, D. Capco, A. Ben Zeev, S. Wittelsberger and C. F. Tse, Cytoplasmic and nuclear architecture in cells and tissue: form, function, and mode of assembly. *Cold Spring Harb. Symp. quant. Biol.* **XLVI**, 1013–1028 (1981).
19. M. Bouteille, D. Bouvier and A. P. Seve, Heterogeneity and territorial organization of the nuclear matrix and related structures. *Int. Rev. Cytol.* **83**, 135–182 (1983).
20. L. Manuelidis, Different central nervous system cell types display distinct and nonrandom arrangements of satellite DNA sequences. *Proc. natn. Acad. Sci. U.S.A.* **81**, 3123–3127 (1984).
21. M. Schliwa, Mechanisms of intracellular organelle transport. In *Cell and Muscle Motility*, Vol. 5 (Edited by J. W. Shaw), pp. 1–82. Plenum, New York (1984).
22. W. G. Nelson, K. J. Pienta, E. R. Barrack and D. S. Coffey, The role of the nuclear matrix in the organization and function of DNA. *A. Rev. Biophys. biophys. chem.* **15**, 457–475 (1986).
23. J. W. Gray, P. N. Dean and M. L. Mendelsohn, Quantitative cell cycle analysis. In *Flow Cytometry and Sorting* (Edited by M. Melamed, P. Mullaney and M. L. Mendelsohn), pp. 383–407. Wiley, New York (1979).
24. C. Rossi, The use of cytofluorimetric data for oncological research: recovering DNA distribution by EM method. In *Proc. 11th IMACS World Congress*, Vol. 3 (Edited by B. Wahlstrom, R. Henriksen and N. P. Sundby), pp. 57–60. Moberg & Helli, Oslo (1985).
25. P. A. Fantes, W. D. Grant, R. H. Pritchard, P. E. Sudbery and A. E. Wheals, The regulation of cell size and the control of mitosis. *J. theor. Biol.* **50**, 213–244 (1975).
26. D. R. Rigney, Correlations between the ages of sibling cell cycle events and a test of the "transition probability" cell cycle model. In *Biomathematics and Cell Kinetics* (Edited by M. Rotenberg), pp. 157–166. Elsevier/North-Holland, Amsterdam (1981).
27. D. R. Rigney, Analysis of bivariate flow cytometry data. In *Biomathematics and Cell Kinetics* (Edited by M. Rotenberg), pp. 375–388. Elsevier/North-Holland, Amsterdam (1981).
28. J. J. Tyson, The coordination of cell growth and division-intentional or incidental? *Bioessays* **2**, 72–77 (1985).
29. M. Kimmel, Z. Darzynkiewicz, O. Arino and F. Traganos, Analysis of a cell cycle model based on unequal division of metabolic constituents to daughter cells during cytokinesis. *J. theor. Biol.* **110**, 637–664 (1984).
30. H. M. Shapiro, *Practical Flow Cytometry*. Liss, New York (1985).
31. B. Trask, G. Van den Engh, J. Landegent, N. J. In de Wal and M. Van der Ploeg, Detection of DNA sequences in nuclei in suspension by *in situ* hybridization and dual beam flow cytometry. *Science* **230**, 1401–1403 (1985).
32. D. A. Cantrell and K. A. Smith, The interleukin-2 T cell sytem: a new cell growth model. *Science* **224**, 1312–1316 (1984).
33. R. F. Brooks, F. N. Richmond, P. N. Riddle and K. M. V. Richmond, Apparent heterogeneity in the response of quiescent swiss 3T3 cells to serum growth factors. *J. cell. Physiol.* **121**, 341–350 (1984).
34. D. R. Rigney, Stochastic model of constitutive protein levels in growing and dividing bacterial cells. *J. theor. Biol.* **76**, 453–480 (1979).
35. D. R. Rigney, Multiple-transition cell cycle models that exhibit transition probability kinetics. *Cell Tiss. Kinet.* **19**, 23–37 (1986).
36. C. W. Birky, The partitioning of cytoplasmic organelles at cell division. *Int. Rev. Cytol. (Suppl.)* **15**, 49–89 (1983).
37. A. B. Pardee, B.-Z. Shilo and A. L. Koch, Variability of the cell cycle. *Cold Spring Harb. Conf. Cell Prolif.* **6**, 373–392 (1979).
38. J. J. Tyson and K. B. Hannsgen, The distribution of cell size and generation time in a model of the cell cycle incorporating size control and random transitions. *J. theor. Biol.* **113**, 29–62 (1985).
39. J. J. Tyson and K. B. Hannsgen, Cell growth and division: global asymptotic stability of the size distribution in probabilistic models of the cell cycle. *J. math. Biol.* **22**, 61–68 (1985).
40. A. Koch and M. Schaechter, A model for the statistics of the cell division process. *J. gen. Microbiol.* **29**, 435–454 (1962).
41. J. A. Smith and L. Martin, Do cells cycle?. *Proc. natn. Acad. Sci. U.S.A.* **70**, 1263–1267 (1973).
42. R. F. Brooks, D. C. Bennett and J. A. Smith, Mammalian cell cycles need two random transitions. *Cell* **19**, 493–504 (1980).
43. K. B. Dawson, H. Madoc-Jones and E. O. Field, Variations in the generation times of a strain of rat sarcoma cells in culture. *Expl Cell Res.* **38**, 75–84 (1965).
44. D. Hemon, M. Collyn-d'Hooghe, A. J. Valleron and E. P. Malaise, Statistical methods for the estimation and analysis of correlations between characteristics of cells observed using time-lapse microcinematography. In *Biomathematics and Cell Kinetics* (Edited by A. J. Valleron and P. D. M. Macdonald), pp. 43–55. Elsevier/North-Holland, Amsterdam (1978).

45. H. Miyamoto, E. Zeuthen and L. Rasmussen, Clonal growth of mouse cells (strain L). *J. Cell Sci.* **13,** 879–888 (1973).
46. M. Collyn-d'Hooghe, A.-J. Valleron and E. P. Malaise, Time lapse cinematography studies of cell cycle and mitosis duration. *Expl Cell Res.* **106,** 405–407 (1977).
47. R. Van Wijk and K. W. Van de Poll, Variability of cell generation times in a hepatoma cell pedigree. *Cell Tiss. Kinet.* **12,** 659–663 (1979).
48. S. Cooper, The continuum model: statistical implications. *J. theor. Biol.* **94,** 783–800 (1982).
49. R. F. Brooks, J. A. Smith, D. C. Bennett and K. V. M. Richmond, G1 rate model of the cell cycle[1]—a realistic alternative to "transition probability"? *Nature* **293,** 680–681 (1981).
50. J. E. Sisken and L. Morasca, Intrapopulation kinetics of mitotic cycle. *J. cell. Biol.* **25,** 179–189 (1965).
51. L. N. Castor, A G1 rate model accounts for cell-cycle kinetics attributed to transition probability. *Nature* **287,** 857–859 (1980).
52. S. I. Rubinow, A maturity-time representation for cell populations. *Biophys. J.* **8,** 1055–1073 (1968).
53. M. Rotenberg, Correlations, asymptotic stability, and the G0 theory of the cell cycle. In *Biomathematics and Cell Kinetics* (Edited by A. J. Valleron and P. D. M. Macdonald), pp. 59–69. Elsevier/North-Holland, Amsterdam (1978).
54. M. Rotenberg, Theory of distributed quiescent state in the cell cycle. *J. theor. Biol.* **96,** 495–509 (1982).
55. M. Rotenberg, Transport theory for growing cell populations. *J. theor. Biol.* **103,** 181–199 (1983).
56. C. Milcarek and K. Zahn, The synthesis of ninety proteins including actin throughout the HeLa cell cycle. *J. Cell Biol.* **79,** 833–838 (1978).
57. R. Bravo and J. E. Celis, A search for differential polypeptide synthesis throughout the cell cycle of HeLa cells. *J. Cell Biol.* **84,** 795–802 (1980).
58. R. Bravo and J. E. Celis, Updated catalog of HeLa cell proteins. *Clin. Chem.* **28,** 766–781 (1982).
59. L. Kaczmarek, B. Calabretta and R. Baserga, Expression of cell-cycle-dependent genes in phytohemagglutinin-stimulated human lymphocytes. *Proc. natn. Acad. Sci. U.S.A.* **82,** 5375–5379 (1985).
60. R. Baserga, *The Biology of Cell Reproduction.* Harvard Univ. Press, Cambridge, Mass. (1985).
61. A. Zetterberg and W. Engstrom, Mitogenic effect of alkaline pH on quiescent serum-starved cells. *Proc. natn. Acad. Sci. U.S.A.* **78,** 4334–4338 (1981).
62. G. A. Koretzky, R. P. Daniele, W. C. Greene and P. C. Nowell, Evidence for an interleukin-independent pathway for human lymphocyte activation. *Proc. natn. Acad. Sci. U.S.A.* **80,** 3444–3447 (1983).
63. D. Mazia, Mitosis and the physiology of cell division. In *The Cell,* Vol. 3 (Edited by J. Brachet and A. E. Mirsky), pp. 77–412. Academic Press, New York (1961).
64. K. Sperling, Cell cycle and chromosome cycle: morphological and functional aspects. In *Premature Chromosome Condensation* (Edited by P. N. Rao, R. T. Johnson and K. Sperling). Academic Press, New York (1982).
65. P. N. Rao, B. Wilson and T. T. Puck, Premature chromosome condensation and cell cycle analysis. *J. Cell Physiol.* **91,** 131–142 (1977).
66. P. N. Rao, R. T. Johnson and K. Sperling (Eds), *Premature Chromosome Condensation. Applications in Basic, Clinical, and Mutation Research.* Academic Press, New York (1982).
67. M. Camargo and J. Cervenka, Patterns of DNA replication of human chromosomes. II. Replication map and replication model. *Am. J. Hum. Genet.* **34,** 757–780 (1982).
68. J. R. K. Savage, R. Prasad and D. G. Papworth, Subdivision of S-phase and its use for comparative purposes in cultured human cells. *J. theor. Biol.* **111,** 355–357 (1984).
69. M. A. Goldman, G. P. Holmquist, M. C. Gray, L. A. Caston and A. Nag, Replication timing of genes and middle repetitive sequences. *Science* **224,** 686–692 (1984).
70. C. Nicolini, F. Kendall and W. Giaretti, Objective identification of cell cycle phases and subphases by automated image analysis. *Biophys. J.* **19,** 163–176 (1977).
71. C. Nicolini, Nuclear morphometry, quinternary chromatin structure and cell growth. *J. submicrosc. Cytol.* **12,** 475–505 (1980).
72. C. Nicolini, Normal versus abnormal cell proliferation—a unitary and analytical overview. *Cell biophys.* **2,** 271–290 (1980).
73. A. Belmont, F. M. Kendall and C. Nicolini, Three-dimensional intranuclear DNA organization *in situ*: three states of condensation and their redistribution as a function of nuclear size near the G1–S border in HeLa S-3 cells. *J. Cell Sci.* **65,** 123–138 (1984).
74. Z. Darzynkiewicz, F. Traganos and M. R. Melamed, New cell cycle compartments identified by multiparameter flow cytometry. *Cytometry* **1,** 98–108 (1980).
75. M. Anastassova-Kristeva, The nucleolar cycle in man. *J. Cell Sci.* **25,** 103–110.
76. R. J. Beckman and M. S. Waterman, On the random distribution of nucleoli in metabolic cells. *J. theor. Biol.* **69,** 561–562 (1977).
77. J. Gani and I. Saunders, Nucleolar aggregation: modelling and simulation. *J. theor. Biol.* **72,** 81–90 (1978).
78. B. Lewin, *Gene Expression 2,* Chap. 27. Wiley, New York (1980).
79. R. P. Perry, RNA processing comes of age. *J. Cell Biol.* **91,** 28s–38s (1981).
80. H. Busch, SNRNAS, SNRNPS and RNA processing. *A. Rev. Biochem.* **51,** 617–654 (1982).
81. G. N. Wilson, The structure and organization of human ribosomal genes. *Cell Nucleus* **10,** 287–318 (1982).
82. M. Nomura, R. Gourse and G. Baughman, Regulation of the synthesis of ribosomes and ribosomal components. *A. Rev. Biochem.* **53,** 75–117 (1984).
83. C. E. Sekeris, The role of HnRNA in the control of ribosomal gene transcription. *J. theor. Biol.* **114,** 601–604 (1985).
84. O. L. Miller, The nucleolus, chromosomes, and visualization of genetic activity. *J. Cell Biol.* **91,** 15s–27s (1981).
85. E. G. Jordan and C. A. Cullis (Eds), *The Nucleolus.* Cambridge Univ. Press, London (1982).
86. H. G. Schwarzacher and F. Wachtler, Nucleolus organizer regions and nucleoli. *Hum. Genet.* **63,** 89–99 (1983).
87. D. Hernandez-Verdun, The nucleolar organizer regions. *Biol. Cell* **49,** 191–202 (1983).
88. G. Goessens, Nucleolar structure. *Int. Rev. Cytol.* **87,** 107–158 (1984).
89. C. Mirre and B. Knibiehler, A reevaluation of the relationships between the fibrillar centers and the nucleolus organizing regions in reticulated nucleoli: ultrastructural organization, number, and distribution of the fibrillar centers in the nucleolus of the mouse Sertoli cell. *J. Cell Sci.* **55,** 247–259 (1982).

90. U. Scheer and K. M. Rose, Localization of RNA polymerase I in interphase cells and mitotic chromosomes by light and electron-microscopic immunocytochemistry. *Proc. natn. Acad. Sci. U.S.A.* **81,** 1431–1435 (1985).
91. G. Chambliss, G. R. Craven, J. Davies, K. Davis, L. Kahan and M. Nomura (Eds), *Ribosomes: Structure, Function, and Genetics*. Univ. Park Press, Baltimore, Md (1980).
92. H. M. Fried and J. R. Warner, Organization and expression of eukaryotic ribosomal protein genes. In *Recombinant DNA and Cell Proliferation* (Edited by G. S. Stein and G. L. Stein), pp. 169–192. Academic Press, New York (1984).
93. J. R. Warner, R. J. Tushinski and P. J. Wejksnora, Coordination of RNA and proteins in eukaryotic ribosome production. In *Ribosomes: Structure, Function, and Genetics* (Edited by G. Chambliss, G. R. Craven, J. Davies, K. Davies, L. Kahan and M. Namura), pp. 889–902. Univ. Park Press, Baltimore, Md (1980).
94. H. Green, Ribosome synthesis during preparation for division in the fibroblast. *Cold Spring Harb. Conf. Cell Prolifn* **1,** 743–755 (1974).
95. S. A. Liebhaber, S. Wolf and D. Schlessinger, Differences in rRNA metabolism of primary and SV40 transformed human fibroblasts. *Cell* **13,** 121–127 (1978).
96. B. P. Brandhorst and E. H. McConkey, Stability of nuclear RNA in mammalian cells. *J. molec. Biol.* **85,** 451–463 (1974).
97. A. L. Goldberg and A. C. St. John, Intracellular protein degradation in mammalian and bacterial cells: Part 2. *A. Rev. Biochem.* **45,** 747–803 (1976).
98. D. M. Pardoll and B. Vogelstein, Sequence analysis of nuclear matrix associated DNA from rat liver. *Expl Cell Res.* **128,** 466–470 (1980).
99. R. Ochs, M. Lischwe, P. O'Leary and H. Busch, Localization of nucleolar phosphoproteins B23 and C23 during mitosis. *Expl Cell Res.* **146,** 139–149 (1983).
100. H. R. Hubbell, Silver staining as an indicator of active ribosomal genes. *Stain Technol.* **60,** 285–294 (1985).
101. Anon., Silver staining of nucleoli and nucleolar organizer regions. Specialty No. 121. In *ISI Atlas of Science: Biotechnology and Molecular Genetics*, pp. 595–597. ISI Press, Philadelphia, Pa (1985).
102. R. Love and R. J. Walsh, Nucleolinar morphology in normal diploid, neoplastic, and aneuploid cells *in vitro*. *Cancer Res.* **30,** 990–997 (1970).
103. R. Love and R. Z. Soriano, Correlation of nucleolini with fine structural nucleolar constituents of cultured normal and neoplastic cells. *Cancer Res.* **31,** 1030–1037 (1971).
104. H. Busch (Ed.) and K. Smetana, The nucleus of the cancer cell. In *The Molecular Biology of Cancer*, pp. 41–80. Academic Press, New York (1974).
105. E. G. Jordan and J. H. McGovern, The quantitative relationship of the fibrillar centers and other nucleolar components to changes in growth conditions serum deprivation and low doses of actinomycin D in cultured diploid human fibroblasts (strain MRC 5). *J. Cell Sci.* **52,** 373–389 (1981).
106. I. Raska, Z. Rychter and K. Smetana, Fibrillar centres and condensed nucleolar chromatin in resting and stimulated human lymphocytes. *Z. mikrosk.-anat. Forsch. Leipzig* **97,** 15–32 (1983).
107. P. Gozak, Y. S. Chentsov and O. V. Zatsepin, Ultrastructure, shape, and number of fibrillar centers in PK cells in the period of G0. *Tsitologiya* **25,** 1236 (1984).
108. J. M. Varley, Patterns of silver staining of human chromosomes. *Chromosoma* **61,** 207–214 (1977).
109. H. Schmiady, M. Muenke and K. Sperling, Ag-staining of NOR regions in human prematurely condensed chromosomes from cells with different ribosomal RNA gene activity. *Expl Cell Res.* **121,** 425–428 (1979).
110. B. R. Reeves, G. Casey, J. R. Honeycombe and S. Smith, Correlation of differentiation state and silver staining of nucleolar organizers in the promyelocytic leukemia cell line HI-60. *Cancer Genet. Cytogenet.* **13,** 159–166 (1984).
111. A. DeCapoa, P. Marlekaj, A. Baldini, N. Archidiacono and M. Rocchi, The transcriptional activity of individual ribosomal DNA gene clusters is modulated by serum concentration. *J. Cell Sci.* **74,** 21–35 (1985).
112. K. G. Miller and B. Sollner-Webb, Transcription of mouse ribosomal RNA genes by RNA polymerase I—*in vitro* and *in vivo* initiation and processing sites. *Cell Nucleus* **12,** 69–100 (1981). [*rDNA*, Part C (Edited by H. Busch and L. Rothblum). Academic Press, New York (1981).]
113. O. J. Miller, R. Tantravahi, R. Katz, B. F. Erlanger and R. V. Guntaka, Amplification of mammalian ribosomal RNA genes and their regulation by methylation. In *Genes, Chromosomes, and Neoplasia* (Edited by F. E. Arrighi, P. N. Rao and E. Stubblefield), pp. 253–270. Raven Press, New York (1981).
114. H. Busch, The current excitement about gene controls of nucleolar rDNA. *Life Sci.* **23,** 2543–2554 (1978).
115. H. Busch and I. L. Goldknopf, Ubiquitin–protein conjugates. *Molec. cell. Biochem.* **40,** 173–187 (1981).
116. H. Busch, Ubiquitination of proteins. *Meth. Enzym.* **106,** 238–262 (1984).
117. L. Levinger and A. Varshavsky, Selective arrangement of ubiquitinated and D1 protein-containing nucleosomes within the *Drosophila* genome. *Cell* **28,** 375–385 (1982).
118. A. Varshavsky, L. Levinger, O. Sundin, J. Barsoum, E. Ozkaynak, P. Swerdlow and D. Finley, Cellular and SV40 chromatin: replication, segregation, ubiquitination, nuclease-hypersensitive sites, HMG-containing nucleosomes, and heterochromatin-specific protein. *Cold Spring Harb. Symp. quant. Biol.* **47,** 511–528 (1983).
119. S. Matsui, B. K. Seon and A. A. Sandberg, Disappearance of a structural chromatin protein A24 in mitosis: implications for molecular basis of chromatin condensation. *Proc. natn. Acad. Sci. U.S.A.* **76,** 6386–6390 (1979).
120. C. P. Prior, C. R. Cantor, E. M. Johnson, V. C. Littau and V. G. Allfrey, Reversible changes in nucleosome structure and H3 accessibility in transcriptionally active and inactive states of rDNA chromatin. *Cell* **34,** 1033–1042 (1983).
121. L. Levinger, J. Barsoum and A. Varshavsky, Two-dimensional hybridization mapping of nucleosomes: comparison of DNA and protein patterns. *J. molec. Biol.* **146,** 287–304 (1981).
122. D. D. Brown, The role of stable complexes that repress and activate eukaryotic genes. *Cell* **37,** 359–365 (1984).
123. M. S. Schlissel and D. D. Brown, The transcriptional regulation of Xenopus 5S RNA genes in chromatin—the roles of active stable transcription complexes and histone H1. *Cell* **37,** 903–913 (1984).
124. D. A. Miller, V. G. Dev, R. Tantravahi and O. J. Miller, Suppression of human nucleolus organizer activity in mouse–human somatic hybrid cells. *Expl Cell Res.* **101,** 235–243 (1976).

125. O. J. Miller, D. A. Miller, V. G. Dev, R. Tantravahi and C. M. Croce, Expression of human and suppression of mouse nucleolus organizer activity in mouse–human somatic cell hybrids. *Proc. natn. Acad. Sci. U.S.A.* **73,** 4531–4535 (1976).
126. C. M. Croce, A. Talavera, C. Basilico and O. J. Miller, Suppression of production of mouse 28S ribosomal RNA in mouse–human hybrids segregating mouse chromosomes. *Proc. natn. Acad. Sci. U.S.A.* **74,** 694–697 (1977).
127. A. Worcel, Molecular architecture of the chromatin fiber. *Cold Spring Harb. Symp. quant. Biol.* **42,** 313–324 (1977).
128. I. L. Goldknopf, M. W. Anderson, N. R. Ballal, G. Wilson and H. Busch, Evidence that protein A-24 may stabilize a potentially active chromatin structure by interlocking nucleosome cores. *Eur. J. Cell Biol.* **22,** 95 (1980).
129. F. D. McKeon, D. L. Tuffanelli, S. Kobayashi and M. W. Kirschner, The redistribution of a conserved nuclear envelope protein during the cell cycle suggests a pathway for chromosome condensation. *Cell* **36,** 83–92 (1984).
130. T. Marunouchi, S. Mita, Y. Matsumoto and H. Yasuda, A temperature sensitive mutant and the nature of G2-mitosis transition. In *Premature Chromosome Condensation* (Edited by P. N. Rao, R. T. Johnson and K. Sperling), pp. 173–194. Academic Press, New York (1982).
131. H. Holzer and P. C. Heinrich, Control of proteolysis. *A. Rev. Biochem.* **49,** 63–91 (1980).
132. A. Hershko and A. Ciechanover, Mechanisms of intracellular protein breakdown. *A. Rev. Biochem.* **51,** 335–364 (1982).
133. A. Hershko, Ubiquitin: roles in protein modification and breakdown. *Cell* **34,** 11–12 (1983).
134. M. Siegelman, M. W. Bond, W. M. Gallatin, T. St John, H. T. Smith, V. A. Fried and I. L. Weissman, Cell surface molecule associated with lymphocyte homing is ubiquitinated branched-chain glycoprotein. *Science* **231,** 823–829 (1986).
135. D. Finley, A. Ciechanover and A. Varshavsky, Thermolability of ubiquitin-activating enzyme from the mammalian cell cycle mutant ts85. *Cell* **37,** 43–55 (1984).
136. A. Ciechanover, D. Finley and A. Varshavsky, Ubiquitin dependence of selective protein degradation demonstrated in the mammalian cell cycle mutant ts85. *Cell* **37,** 57–66 (1984).
137. Z. Darzynkiewicz, D. P. Evenson, L. Staiano-Coico, T. K. Sharpless and M. L. Melamed, Correlation between cell cycle duration and RNA content. *J. cell. Physiol.* **100,** 425–438 (1979).
138. K. F. Fujikawa-Yamamoto, RNA dependence in the cell cycle of V79 cells. *J. cell. Physiol.* **112,** 60–66 (1982).
139. R. Baserga, Growth in size and cell DNA replication. *Expl Cell Res.* **151,** 1–5 (1984).
140. A. Zetterberg and W. Engstrom, Induction of DNA synthesis and mitosis in the absence of cellular enlargement. *Expl Cell Res.* **144,** 199–207 (1983).
141. A. Zetterberg, W. Engstrom and E. Dafgard, The relative effects of different types of growth factors on DNA replication, mitosis, and cellular enlargement. *Cytometry* **5,** 368–375 (1984).
142. M. Das, Epidermal growth factor: mechanisms of action. *Int. Rev. Cytol.* **78,** 233–256 (1982).
143. J. Zapf, E. R. Froesch and R. E. Humbel, The insulin-like growth factors (IGF) of human serum: chemical and biological characterization and aspects of their possible physiological role. *Curr. Top. Cell Regul.* **19,** 257–309 (1981).
144. R. G. Ham, Growth of human fibroblast cultures in serum-free medium. In *Methods for Serum-free Culture of Epithelial and Fibroblastic Cells.* (Edited by D. W. Barnes), pp. 249–264. Liss (1984).
145. G. K. Haselbacher, R. E. Humbel and G. Thomas, Insulin-like growth factor: insulin or serum increase phosphorylation of ribosomal protein S6 during transition of stationary chick embryo fibroblasts into early G1 phase of the cell cycle. *FEBS Lett.* **100,** 185–190 (1979).
146. J. Gordon, P. J. Nielsen, K. L. Manchester, H. Towbin, L. Jimenez de Asua and G. Thomas, Criteria for establishment of the biological significance of ribosomal protein phosphorylation. *Curr. Topics Cell. Regul.* **21,** 89–99 (1982).
147. I. Novak-Hofer and G. Thomas, An activated S6 kinase in extracts from serum and epidermal growth factor stimulated Swiss 3T3 cells. *J. biol. Chem.* **259,** 5995–6000 (1984).
148. J. Pouyssegur, J. C. Chambard, A. Franchi, S. Paris and E. Van Obberghen-Schilling, Growth factor activation of an amiloride-sensitive Na/H exchange system in quiescent fibroblasts: coupling to ribosomal protein S6 phosphorylation. *Proc. natn. Acad. Sci. U.S.A.* **79,** 3935–3939 (1982).
149. D. Lloyd, R. K. Poole and S. W. Edwards, *The Cell Divison Cycle. Temporal Organization and Control of Cellular Growth and Reproduction.* Academic Press, London (1982).
150. M. Wintzerith, E. Wittendorp, M. E. Ittel, R. V. Rechenmann and P. Mandel, Track autoradiographic study of nucleolar DNA synthesis in adult rat liver. *Expl Cell Res.* **91,** 279–284 (1975).
151. F. Amaldi, D. Giacomoni and R. Zito-Bignami, On the duplication of ribosomal RNA cistrons in Chinese hamster ovary cells. *Eur. J. Biochem.* **11,** 419–423 (1969).
152. P. J. Stambrook, The temporal replication of ribosomal genes in synchronized Chinese Hamster cells. *J. molec. Biol.* **82,** 303–313 (1974).
153. I. Balazs and C. L. Schildkraut, DNA replication in synchronized cultured mammalian cells. *J. molec. Biol.* **57,** 153–158 (1971).
154. I. Balazs and C. L. Schildkraut, DNA replication in synchronized cultured mammalian cells. VI. The temporal replication of ribosomal cistrons in synchronized cell lines. *Expl Cell Res.* **101,** 307–314 (1976).
155. A. Zellweger, U. Ryser and R. Braun, Ribosomal genes of physarum: their isolation and replication in the mitotic cycle. *J. molec. Biol.* **64,** 681–691 (1972).
156. D. Giacomoni and D. Finkel, Time of duplication of ribosomal RNA cistrons in a cell line of potorous tridactylis (rat kangaroo). *J. molec. Biol.* **70,** 725–728 (1972).
157. G. M. Gimmler and E. Schweizer, rDNA replication in a synchronized culture of Saccharomyces cerevisiae. *Biochem. Biophys. Res. Commun.* **46,** 143–149 (1972).
158. C. S. Newlon, G. E. Sonenshein and C. E. Holt, Time of synthesis of genes for ribosomal ribonucleic acid in *Physarum. Biochemistry* **12,** 2338–2345 (1973).
159. E. Epner, R. A. Rifkind and P. A. Marks, Replication of alpha and beta globin DNA sequences occurs during early S phase in murine leukemia cells. *Proc. natn. Acad. Sci. U.S.A.* **78,** 3058–3062 (1981).
160. A. Rode, C. de Taisne and C. Hartmann, Incorporation of 5-bromodeoxyuridine in the total and ribosomal DNA of synchronously dividing chick embryo fibroblasts. *Experientia* **39,** 1134–1136 (1983).

161. A. O. D'Andrea, U. Tantravahi, M. Lalande, M. A. Perle and S. A. Latt, High resolution analysis of the timing of replication of specific DNA sequences during S phase of mammalian cells. *Nucleic Acid Res.* **11,** 4753–4774 (1983).
162. M. Bobrow and J. Heritage, Nonrandom segregation of nucleolar organizing chromosomes at mitosis? *Nature* **288,** 79–81 (1980).
163. R. J. Strobel, S. Pathak and T. C. Hsu, NOR lateral asymmetry and its effect on satellite association in BrdU-labeled human lymphocyte cultures. *Hum. Genet.* **59,** 259–262 (1981).
164. J. Cairns, Mutation selection and the natural history of cancer. *Nature* **255,** 197–200 (1975).
165. C. S. Potten, W. J. Hume, P. Reid and J. Cairns, The segregation of DNA in epithelial cells. *Cell* **15,** 899–906 (1978).
166. P. Jablonka and E. Jablonka, Non-random sister chromatid segregation by cell type. *J. theor. Biol.* **99,** 427–436 (1982).
167. G. Nicolis and I. Prigogine, *Self-organization in Nonequilibrium Systems.* Wiley, New York (1977).
168. N. G. Van Kampen, *Stochastic Processes in Physics and Chemistry.* North-Holland, Amsterdam (1982).
169. W. Feller, *An Introduction to Probability Theory and Its Applications.* Wiley, New York (1957).
170. D. G. Kendall, On the role of variable generation time in the development of a stochastic birth process. *Biometrika* **35,** 316–330 (1948).
171. M. Takahashi, Theoretical basis for cell cycle analysis. *J. theor. Biol.* **18,** 195–209 (1968).
172. J. W. Gray, Cell cycle analysis of perturbed cell populations. *Cell Tiss. Kinet.* **9,** 499–516 (1976).
173. P. R. Painter and A. G. Marr, Mathematics of microbial populations. *A. Rev. Microbiol.* **22,** 519 (1968).
174. P. D. M. Macdonald, On the statistics of cell proliferation. In *The Mathematical Theory of the Dynamics of Biological Populations* (Edited by M. S. Bartlett and R. W. Hiorns), pp. 303–314. Academic Press, New York (1973).
175. P. D. M. Macdonald, Age distribution in the general kinetic model. In *Biomathematics and Cell Kinetics* (Edited by A. J. Valleron and P. D. M. Macdonald), p. 3–20. Elsevier/North-Holland, Amsterdam (1978).
176. E. O. Powell, Generation times of bacteria: real and artificial distributions. *J. gen. Microbiol.* **58,** 141–144 (1969).
177. P. R. Painter, Generation times of bacteria. *J. gen. Microbiol.* **89,** 217–220 (1975).
178. R. Staudte and R. Cowan, Models for dependent cell data. In *Proc. 11th IMACS World Congress,* Vol. 3 (Edited by B. Wahlstrom, R. Henriksen and N. P. Sundby), pp. 85–88. Moberg & Helli, Oslo (1985).
179. R. M. Shymko and R. R. Klevecz, Cell division gated by oscillatory time keeping and critical size. In *Biomathematics and Cell Kinetics* (Edited by M. Rotenberg), pp. 329–348. Elsevier/North-Holland, Amsterdam (1981).
180. R. R. Klevecz and R. M. Shymko, Quasi-exponential generation time distributions from a limit cycle oscillator. *Cell Tiss. Kinet.* **18,** 263–271 (1985).
181. V. I. Arnold, *Ordinary Differential Equations.* MIT Press, Cambridge, Mass. (1978).
182. G. G. Steel, *Growth Kinetics of Tumors.* Clarendon Press, Oxford (1977).
183. W. A. Aherne, R. S. Camplejohn and N. A. Wright, *An Introduction to Cell Population Kinetics.* Univ. Park Press, Baltimore, Md (1977).
184. N. R. Hartman, C. W. Gilbert, B. Jansson, P. D. M. Macdonald, G. G. Steel and A. J. Valleron, A comparison of computer methods for analysis of fraction labelled mitoses curves. *Cell Tiss. Kinet.* **8,** 119–124 (1975).
185. E. O. Voit and G. Dick, Growth of cell populations with arbitrarily distributed cycle durations. II. Extended model for correlated cycle durations of mother and daughter cells. *Maths Biosci.* **66,** 247–262 (1983).
186. R. H. Herzig, S. N. Wolff, H. M. Lazarus, G. L. Phillips, C. Karanes and G. P. Herzig, High-dose cytosine arabinoside therapy for refractory leukemia. *Blood* **62,** 361–369 (1983).
187. J. M. Venditti, Treatment schedule dependency of experimentally active antileukemic (L1210) drugs. *Cancer Chemother Rep.* **2,** 35–59 (1971).
188. S. I. Rubinow and J. L. Lebowitz, A mathematical model of the chemotherapeutic treatment of acute myeloblastic leukemia. *Biophys. J.* **16,** 1257–1271 (1976).
189. G. W. Swan, *Some Current Mathematical Topics in Cancer Research.* Univ. Microfilms International, Ann Arbor, Mich. (1977).
190. C. M. Newton, Biomathematics in oncology: modeling of cellular systems. *A. Rev. Biophys. Bioengng* **9,** 541–579 (1980).
191. B. F. Dibrov, A. M. Zhabotinsky, Y. A. Neyfakh, M. P. Orlova and L. I. Churikova, Mathematical model of cancer chemotherapy. Periodic schedules of phase-specific cytotoxic-agent administration increasing the selectivity of therapy. *Maths Biosci.* **73,** 1–31 (1985).
192. I. Tannock, Cell kinetics and chemotherapy: a critical review. *Cancer Treat. Rep.* **62,** 1117–1133 (1978).
193. F. Halberg, E. Haus and L. E. Scheving, Sampling of biological rhythms, chronocytokinetics, and experimental oncology. In *Biomathematics and Cell Kinetics* (Edited by A. J. Valleron and P. D. M. Macdonald), pp. 175–190. Elsevier/North-Holland, Amsterdam (1978).
194. W. J. M. Hrushesky, Circadian timing of cancer chemotherapy. *Science* **228,** 73–75 (1985).
195. T. E. Wheldon, Optimal control strategies in the radiotherapy of human cancer. In *Biomathematics and Cell Kinetics* (Edited by A. J. Valleron and P. D. M. Macdonald), pp. 345–354. Elsevier/North-Holland, Amsterdam (1978).
196. R. E. Peschel and J. J. Fischer, Optimization of the time-dose relationship. *Semin. Oncol.* **8,** 38–48 (1981).
197. M. Edelstein, T. Vietti and F. Valeriote, Schedule-dependent synergism for the combination of 1-β-D-arabinofuranosylcytosine and daunorubicin. *Cancer Res.* **34,** 293–297 (1974).
198. M. Y. Chu and G. A. Fischer, The incorporation of ^{3}H-cytosine arabinoside and its effect on murine leukemia cells (L5178Y). *Biochem. Pharmac.* **17,** 753–767 (1968).
199. M. Y. Chu, Incorporation of arabinosyl cytosine into 2-7S ribonucleic acid and cell death. *Biochem. Pharmac.* **20,** 2057–2063 (1971).
200. M. Takahashi, Theoretical basis for cell cycle analysis. 1. Labeled mitosis wave method. *J. theor. Biol.* **13,** 202–211 (1966).
201. R. A. White, S. L. Rasmussen and H. D. Thames, State vector models of the cell cycle. III. Continuous time cell cycle models *J. theor. Biol.* **81,** 181–200 (1979).
202. A. Bertuzzi, A. Gandolfi and M. A. Giovenco, Mathematical models of the cell cycle with a view to tumor studies. *Maths Biosci.* **53,** 159–188 (1981).

203. L. Alberghina and L. Mariani, Control of cell growth and division. In *Biomathematics and Cell Kinetics* (Edited by A. J. Valleron and P. D. M. Macdonald), pp. 89–102. Elsevier/North-Holland, Amsterdam (1978).
204. J. L. Hopper and P. J. Brockwell, A stochastic model for cell populations with circadian rhythms. *Cell Tiss. Kinet.* **11,** 205–225 (1978).
205. J. Hopper and P. Brockwell, Analysis of data from cell populations with circadian rhythms. In *Biomathematics and Cell Kinetics* (Edited by A. J. Valleron and P. D. M. Macdonald), pp. 211–221. Elsevier/North-Holland, Amsterdam (1978).
206. J. A. Hokanson, B. W. Brown, J. R. Thompson and B. Drewinko, Mathematical model for human myeloma relating growth kinetics and drug resistance. *Cell Tiss. Kinet.* **19,** 1–10 (1986).
207. A. Pacault and C. Vidal (Eds), *Non-linear Phenomena in Chemical Dynamics*. Springer, Berlin (1981).
208. H. C. Berg, *Random Walks in Biology*. Princeton Univ. Press, Princeton, N.J. (1983).
209. D. Lauffenburger and C. DeLisi, Cell surface receptors: physical chemistry and cellular regulation. *Int. Rev. Cytol.* **84,** 269–302 (1983).
210. A. Cooper, Protein fluctuations and the thermodynamic uncertainty principle. *Prog. Biophys. molec. Biol.* **44,** 181–214 (1984).
211. H. M. Fishman, Relaxations, fluctuations, and ion transfer across membranes. *Prog. Biophys. molec. Biol.* **46,** 127–162 (1985).
212. K. Cooper, E. Jakobsson and P. Wolynes, The theory of ion transport through membrane channels. *Prog. Biophys. molec. Biol.* **46,** 51–96 (1985).
213. M. B. Rotman, Partial loss of activity of individual molecules of aged beta-galactosidase. In *The Lactose Operon* (Edited by J. R. Beckwith and D. Zipser), pp. 279–289. Cold Spring Harbor Lab., Cold Spring Harbor, N.Y. (1970).
214. B. V. Bronk, G. J. Dienes and A. Paskin, The stochastic theory of cell proliferation. *Biophys. J.* **8,** 1353–1398 (1968).
215. J. C. Angello and J. W. Prothero, Clonal attenuation in chick embryo fibroblasts. *Cell Tiss. Kinet.* **18,** 27–43 (1985).
216. P. Michaelis, Uber Gesetzmassigkeiten des Plasmon-Umkombination und uber eine Methode zur Trennung einer Plastiden, Chondriosomen-, resp. Sphaerosomen-(Mikrosomen)- und einer Zygoplasma-Verebung. *Cytologia* **20,** 315–338 (1955).
217. O. G. Berg, A model for the statistical fluctuations of protein numbers in a microbial population. *J. theor. Biol.* **71,** 587–603 (1978).
218. T. F. Anderson and E. Lustbader, Inheritability of plasmids and populations dynamics of cultured cells. *Proc. natn. Acad. Sci. U.S.A.* **72,** 4085–4089 (1975)
219. T. Williams, The distribution of inanimate marks over a non-homogeneous birth–death process. *Biometrika* **56,** 225–228 (1969).
220. N. M. Yanev and A. Y. Yakovlev, On the distribution of marks over a proliferating cell population obeying the Bellman–Harris branching process. *Maths Biosci.* **75,** 159–173 (1985).
221. B. S. Kerem, R. Goitein, G. Diamond, H. Cedar and M. Marcus, Mapping DNAase I sensitive regions on mitotic chromosomes. *Cell* **38,** 493–499 (1984).
222. M. T. Kuo and W. Plunkett, Nick-translation of metaphase chromosomes. *Proc. natn. Acad. Sci. U.S.A.* **82,** 854–858 (1985).
223. A. J. Coldman and J. H. Goldie, A model for the resistance of tumor cells to cancer chemotherapeutic agents. *Maths Biosci.* **65,** 291–307 (1983).
224. A. J. Coldman, J. H. Goldie and V. Ng, The effect of cellular differentiation on the development of permanent drug resistance. *Maths Biosci.* **74,** 177–198 (1985).
225. D. R. Cox and D. Oakes, *Analysis of Survival Data*. Chapman Hall, London (1984).
226. W. P. Elderton, *Frequency Curves and Correlations*, 4th edn. Harren Press, Washington, D.C. (1953).
227. B. Davies and B. Martin, Numerical inversion of the Laplace transform: a survey and comparison of methods. *J. comput. Phys.* **33,** 1–32 (1979).
228. P. Jagers, Balanced exponential growth: what does it mean and when is it there? In *Biomathematics and Cell Kinetics* (Edited by A. J. Valleron and P. D. M. Macdonald), pp. 21–29. Elsevier/North-Holland, Amsterdam (1978).
229. A. Lasota and M. C. Mackey, Globally asymptotic properties of proliferating cell populations. *J. math. Biol.* **19,** 43–62 (1984).
230. O. Diekmann, H. Heijmans and H. Thieme, On the stability of cell size distributions. *J. math. Biol.* **18,** 135–148 (1984).
231. O. Arino and M. Kimmel, Asymptotic analysis of a cell-cycle model based on unequal cell division. Preprint (1986).
232. G. F. Webb, An operator-theoretic formulation of asynchronous exponential growth. Preprint (1986).
233. B. Klein and A. J. Valleron, A compartmental model for the study of diurnal rhythms in cell proliferation. *J. theor. Biol.* **64,** 27–42 (1977).
234. M. Guiguet, B. Klein and A. J. Valleron, Diurnal variation and the analysis of percent labelled mitosis curves. In *Biomathematics and Cell Kinetics* (Edited by A. J. Valleron and P. D. M. Macdonald), pp. 191–198. Elsevier/North-Holland, Amsterdam (1978).
235. B. Klein and M. Guiguet, Relative importance of the phases of the cell cycle for explaining diurnal rhythms in cell proliferation in the tissues with a long G1 duration. In *Biomathematics and Cell Kinetics* (Edited by A. J. Valleron and P. D. M. Macdonald), pp. 199–210. Elsevier/North-Holland, Amsterdam (1978).
236. N. R. Hartman and U. Moller, A compartment theory in the cell kinetics including considerations on circadian variations. In *Biomathematics and Cell Kinetics* (Edited by A. J. Valleron and P. D. M. Macdonald), pp. 223–251. Elsevier/North-Holland, Amsterdam (1978).
237. O. Diekmann, H. Heijmans and H. R. Thieme, On the stability of cell size distributions. II. Time-periodic developmental rates. Preprint (1986).
238. E. Kamke, *Differentialgleichungen, Lösungsmethoden und Lösungen*, Vol. 1. Chelsea, New York (1948).
239. E. Coddington and N. Levinson, *Theory of Ordinary Differential Equations*, pp. 78–80. McGraw-Hill, New York (1955).
240. A. Stokes, A Floquet theory for functional differential equations. *Science* **48,** 1330–1334 (1962).

APPENDIX A

Master and Moment Equations for the Population

Equations (1a–d) define a stochastic model of the cell cycle, in which the state of each cell is specified by two numbers: X (ranging from 0 to X_{max}) and Y (ranging from 0 to Y_{max}). The state of the cell population is simply the number of cells in each of the $(X_{max}+1)$ $(Y_{max}+1)$ states:

$$\begin{bmatrix} N_{0,0} & \cdots & N_{X,0} & \cdots & N_{X_{max},0} \\ \vdots & & \vdots & & \vdots \\ N_{0,Y} & \cdots & N_{X,Y} & \cdots & N_{X_{max},Y} \\ \vdots & & \vdots & & \vdots \\ N_{0,Y_{max}} & \cdots & N_{X,Y_{max}} & \cdots & N_{X_{max},Y_{max}} \end{bmatrix}.$$

These random variables may assume any conceivable set of integer values $\{n_{0,0}, n_{0,1}, \ldots, n_{X_{max},Y_{max}}\}$, which will have a probability of occurrence $P(N_{0,0}=n_{0,0}, N_{0,1}=n_{0,1}, \ldots, N_{X_{max},Y_{max}}=n_{X_{max},Y_{max}}; t)$ at time t. The master equation describes the rate at which these probabilities change. It is an enumeration of all the ways in which the population may change, as specified by equations (1a–d):

$$\begin{aligned}\frac{d}{dt}P(n_{0,0}, n_{0,1}, \ldots, n_{X_{max},Y_{max}}; t) &= \sum_{y=0}^{Y_{max}} \beta y(n_{X_{max},y}+1)P(n_{0,0}, \ldots, n_{0,y}-2, \ldots, n_{X_{max},y}+1, \ldots, n_{X_{max},Y_{max}}) \\ &+ \sum_{x=0}^{X_{max}-1}\sum_{y=0}^{Y_{max}} \beta y(n_{x,y}+1)P(n_{0,0}, \ldots, n_{x,y}+1, n_{x+1,y}-1, \ldots, n_{X_{max},Y_{max}}) \\ &+ \sum_{x=0}^{X_{max}}\sum_{y=0}^{Y_{max}} \lambda(Y_{max}-y)(n_{x,y}+1)P(n_{0,0}, \ldots, n_{x,y}+1, n_{x,y+1}-1, \ldots, n_{X_{max},Y_{max}}) \\ &+ \sum_{x=0}^{X_{max}}\sum_{y=0}^{Y_{max}} \mu y(n_{x,y}+1)P(n_{0,0}, \ldots, n_{x,y-1}-1, n_{x,y}+1, \ldots, n_{X_{max},Y_{max}}) \\ &- \sum_{x=0}^{X_{max}}\sum_{y=0}^{Y_{max}} [\beta y+\lambda(Y_{max}-y)+\mu y]n_{x,y}P(n_{0,0}, \ldots, n_{X_{max},Y_{max}}). \end{aligned} \tag{A.1}$$

The standard method for solving an equation of this type is to transform it to an equivalent expression in terms of its generating function, defined as

$$\begin{aligned}G(z_{0,0}, z_{0,1}, \ldots, z_{X_{max},Y_{max}}) = \sum_{n_{0,0}=0}^{\infty}\sum_{n_{0,1}=0}^{\infty}\cdots\sum_{n_{x,y}=0}^{\infty}\cdots\sum_{n_{X_{max},Y_{max}}=0}^{\infty} \\ P(n_{0,0}, \ldots, n_{x,y}, \ldots, n_{X_{max},Y_{max}}) z_{0,0}^{n_{0,0}} z_{0,1}^{n_{0,1}} \cdots z_{X_{max},Y_{max}}^{n_{X_{max},Y_{max}}}. \end{aligned} \tag{A.2}$$

Combining equations (A.1) and (A.2), we obtain the result

$$\begin{aligned}\frac{\partial G}{\partial t} = \sum_{y=0}^{Y_{max}} \Bigg\{ \beta y(z_{0,y}^2 - z_{X_{max},y})\frac{\partial G}{\partial z_{X_{max},y}} + \sum_{x=0}^{X_{max}-1} \beta y(z_{x+1,y}-z_{x,y})\frac{\partial G}{\partial z_{x,y}} \\ + \sum_{x=0}^{X_{max}} [\lambda(Y_{max}-y)(z_{x,y+1}-z_{x,y}) + \mu y(z_{x,y-1}-z_{x,y})]\frac{\partial G}{\partial z_{x,y}} \Bigg\}. \end{aligned} \tag{A.3}$$

This partial differential equation is intractable, except for special cases. See Kendall's [170] discussion of the gamma function model, which is a special case in which $\lambda = \mu = 0$. However, the generating function is nevertheless useful because it is more convenient to construct moment equations with equation (A.3) than with the untransformed master equation (A.1). The moment equations are found by taking derivatives of equation (A.3) with respect to the $z_{x,y}$ and evaluating the results at $\{z_{x,y}=1\}$. The reader may verify that the first derivatives of equation (A.3) with respect to the $z_{x,y}$, evaluated at $\{z_{x,y}=1\}$, yield equations that are identical to the deterministic equations given in equations (2a, b). Similarly, the second derivatives of equation (A.3) with respect to the $z_{x,y}$, evaluated at $\{z_{x,y}=1\}$, provide kinetic equations for the variances and correlations between the $N_{x,y}$. Note that if the transition probabilities of equations (1a–d) were not linear functions of the random variables X and Y, the first moment equations would contain terms involving the second moments. Furthermore, the second moment equations would contain terms involving the third moments etc., so that a hierarchy of moment equations would have to be solved to find even the first moments.

If the population begins with $N_{tot}(0)$ cells, each of these cells will produce clones whose size is random. Since the clones are thought to evolve independently of one another, the coefficient of variation of the total population size, $N_{tot}(t)$, will be proportional to $\{N_{tot}(0)\}^{-1/2}$, and stochastic aspects of population growth will be negligible when $N_{tot}(0)$ is large. The evolution of the population may be deterministic even if its initial size is small. Kendall [170] showed that if X_{max} is large (and if the fluctuations in Y are small), then the coefficient of variation in $N_{tot}(t)$ is proportional to $(X_{max}+1)^{-1/2}$. Figures 7 and 10 show how the coefficient of variation of intermitotic times behaves as a function of X_{max} for the bivariate model.

APPENDIX B

Method for Solving for the Distribution of Fibrillar Centers

The distribution in number of activated rDNA genes, $f(\cdot, y; \infty)$, and the Malthusian parameter of exponential growth k, satisfy equation (12). (In what follows, the fractions refer to the "steady state", but we omit the ∞ to simplify the

notation.) The equation may be solved iteratively using the following method. Let the Malthusian parameter k equal some initial guess, say 1. Then iteratively perform the following calculation. Let $f(\cdot, 0) = 1$ initially, so that $f(\cdot, 1)$ may be evaluated:

$$f(\cdot, 1) = \frac{k + \lambda Y_{\max}}{\mu} f(\cdot, 0). \tag{B.1}$$

Similarly, once $f(\cdot, 1)$ is known, the remaining $f(\cdot, y)$ may be evaluated:

$$f(\cdot, y) = \frac{-\lambda[Y_{\max} - (y-2)]f(\cdot, y-2) + \left\{k + \lambda[Y_{\max} - (y-1)] + \mu(y-1) - \beta\left(\frac{1}{\Omega} - 1\right)(y-1)\right\}}{\mu y} f(\cdot, y-1). \tag{B.2}$$

If the calculation with a given estimate of k gives a negative value for any of the $f(\cdot, y)$, set that value equal to zero. Then, when all of the $f(\cdot, y)$ have been calculated, normalize them and calculate the mean value of y. The new guess for k is then set equal to $\beta[(1/\Omega) - 1]$ times this average, for the next iteration.

This procedure is motivated by the following observation. By averaging equation (12) over y we find that the Malthusian growth parameter k is proportional to the average value of y:

$$k = \beta\left(\frac{1}{\Omega} - 1\right)\langle Y \rangle. \tag{B.3}$$

Similarly, by multiplying equation (12) by y and averaging over y, we find the variance in y:

$$\mathrm{var}(y) = \frac{\langle Y \rangle - \frac{\lambda}{\lambda + \mu} Y_{\max}}{\frac{\beta}{\lambda + \mu}\left(\frac{1}{\Omega} - 1\right)}. \tag{B.4}$$

Note that in the limit that β is much smaller than λ and μ, the distribution for Y becomes the binomial given by equation 24(b) with average $\lambda Y_{\max}/(\lambda + \mu)$, so that equation (B.4) becomes an indeterminate form.

APPENDIX C

Moments for the Distribution of Generation Times

The generating function given by equation (23) determines the distribution of cell generation times, among all cells that begin their lives with a specified number of activated rDNA genes, y_0. In this appendix we use that equation to derive arbitrary moments for the distribution. The first two moments are all that are needed for calculating the correlation between sibling, mother and daughter generation times. For the model under investigation, knowledge of all of the moments is sufficient to reconstruct the entire distribution for the first passage time to the state $X = X_{\max} + 1$, i.e. cell division, so that the distribution of generation times is effectively determined. Alternatively, knowledge of the first four moments may be sufficient to recover the distribution approximately [226].

Transition from $X = 0$ to $X = 1$

Since the master equation (16) describes a Markov process, the time spent at each X value, conditioned by the value of Y that it had when the cell first achieved that value of X, is independent of the past history of the cell. Then, transitions from any X to $X + 1$ may be treated the same as that from $X = 0$ to $X = 1$, and the entire cell cycle is simply the convolution of $X_{\max} + 1$ such transitions. Consider the time required to undergo the transition from $X = 0$ to $X = 1$, given that the initial value of Y is y_0. The probability that a cell is in the state $(0, y)$ at age a, given that Y was initially y_0, is obtained by expanding equation (23) in powers of v and by setting $u = 0$. To perform the expansion, note from equations (20a) and (21a, b) that v enters only as the first power, for $Y_{\max} = 1$. Let

$$\begin{aligned} G(r_\pm(u), v; a, 0, Y_{\max} = 1) &= c_0 + d_0 v, \\ G(r_\pm(u), v; a, 1, Y_{\max} = 1) &= c_1 + d_1 v, \end{aligned} \tag{C.1a}$$

where

$$\begin{aligned} c_0 &= c_{0\lambda}\exp(-\lambda a) + c_{0+}\exp(a r_+) + c_{0-}\exp(a r_-), \\ d_0 &= d_{0+}\exp(a r_+) + d_{0-}\exp(a r_-), \\ c_1 &= c_{1+}\exp(a r_+) + c_{1-}\exp(a r_-), \\ d_1 &= d_{1+}\exp(a r_+) + d_{1-}\exp(a r_-) \end{aligned} \tag{C.1b}$$

and

$$\begin{aligned} &c_{0\lambda} = 1 + \frac{\lambda\mu}{(r_+ + \lambda)(r_- + \lambda)}, \quad c_{0+} = \frac{\lambda\mu}{(r_+ + \lambda)(r_+ - r_-)}, \quad c_{0-} = \frac{\lambda\mu}{(r_- + \lambda)(r_- - r_+)}, \\ &c_{1+} = \frac{\mu}{r_+ - r_-}, \quad c_{1-} = \frac{\mu}{r_- - r_+}, \quad d_{1+} = \frac{\lambda + r_+}{r_+ - r_-}, \\ &d_{1-} = \frac{\lambda + r_-}{r_- - r_+}, \quad d_{0+} = \frac{\lambda}{r_+ - r_-}, \quad d_{0-} = \frac{\lambda}{r_- - r_+}. \end{aligned} \tag{C.1c}$$

Then equation (23) becomes

$$G(r_{\pm}(u),\, v;\, \boldsymbol{a},\, y_0,\, Y_{\max} \neq 1) = \sum_{i=0}^{Y_{\max}-y} \sum_{j=0}^{y_0} \frac{(Y_{\max}-y_0)!\,y_0!}{(Y_{\max}-y_0-i)!\,i!(y_0-j)!\,j!} c_0^{Y_{\max}-y_0-i} c_1^{y_0-j} d_0^i d_1^j v^{i+j}. \tag{C.2}$$

By noting the definition of the generating function (17), the values of $P(0, y; \boldsymbol{a}, y_0)$ are obtained by picking out the terms involving v^y and evaluating $c_0(r_{\pm}(u), \boldsymbol{a})$, $d_0(r_{\pm}(u), \boldsymbol{a})$, $c_1(r_{\pm}(u), \boldsymbol{a})$ and $d_1(r_{\pm}(u), \boldsymbol{a})$ at $u = 0$:

$$P(0, y; \boldsymbol{a}, y_0) = \sum_{k=0}^{y} \frac{(Y_{\max}-y_0)!\,y_0!}{(Y_{\max}-y_0-k)!\,k![y_0-(y-k)]!(y-k)!} c_0^{Y_{\max}-y_0-k} c_1^{y_0-(y-k)} d_0^k d_1^{y-k}. \tag{C.3}$$

Having found the probability that the cell be in the $(0, y)$ state as a function of age, given that its initial Y value was y_0, we are in a position to evaluate the following integral for the jth moment of the age when the cell makes the transition from $X = 0$ to $X = 1$:

$$M^{(j)}(y_0 \to y) = \int_0^{\infty} P(0, y; \boldsymbol{a}, y_0) \boldsymbol{a}^j (\beta y\, \mathrm{d}\boldsymbol{a}). \tag{C.4}$$

For $j = 0$, the integral gives the probability that a cell is in the state $(0, y)$ at some age $\boldsymbol{a}$ and then makes the transition to $(1, y)$ over the next infinitesimal time interval, integrated over all possible ages when the transition may occur. That is to say, it is the probability that the cell make the transition from $X = 0$ to $X = 1$ with the indicated value of y:

$$\Pi[(0, y_0) \to (1, y)] \equiv M^{(0)}(y_0 \to y). \tag{C.5}$$

For $j > 0$, the integral gives the expected powers of the ages when the cell makes the transition with the indicated value of y:

$$\langle \{A[(0, y_0) \to (1, y)]\}^j \rangle = \frac{M^{(j)}(y_0 \to y)}{\Pi[(0, y_0) \to (1, y)]}. \tag{C.6}$$

Alternatively, we may consider the moment generating function, which is defined as follows:

$$L(y_0 \to y) \equiv \langle \exp(\boldsymbol{a}s) \rangle = \int_0^{\infty} P(0, y; \boldsymbol{a}, y_0) \exp(\boldsymbol{a}s) (\beta y\, \mathrm{d}\boldsymbol{a}). \tag{C.7a}$$

If the moment generating function is known, the jth moment may be recovered with the aid of the expression

$$M^{(j)}(y_0 \to y) = \frac{\mathrm{d}^j}{\mathrm{d}s^j} L(y_0 \to y)\bigg|_{s=0}. \tag{C.7b}$$

The integrals in equations (C.4) and (C.7a, b) are performed by substituting equation (C.1c) into equation (C.3), by expanding the terms with exponentials, and by integrating the exponentials involving $\boldsymbol{a}$. Both integrals are of the form

$$\begin{aligned} M^{(j)}(y_0 \to y) \quad \text{or} \quad L(y_0 \to y) = \beta y \sum_{i=0}^{y} & \frac{(Y_{\max}-y_0)!\,y_0!}{(Y_{\max}-y_0-i)!\,i![y_0-(y-i)]!(y-i)!} \\ & \times \sum_{k=0}^{Y_{\max}-y_0-i} \frac{(Y_{\max}-y_0-i)!}{k!(Y_{\max}-y_0-i-k)!} \sum_{l=0}^{k} \frac{k!}{(k-l)!\,l!} \\ & \times \sum_{m=0}^{y_0-(y-i)} \frac{[y_0-(y-i)]!}{m![y_0-(y-i)-m]!} \sum_{n=0}^{i} \frac{i!}{n!(i-n)!} \sum_{p=0}^{y-i} \frac{(y-i)!}{p!(y-i-p)!} \\ & \times c_{0\lambda}^{Y_{\max}-y_0-i-k} c_{0+}^{k-l} c_{0-}^{l} c_{1+}^{m} c_{1-}^{y_0-(y-i)-m} d_{0+}^{n} d_{0-}^{i-n} d_{1+}^{p} d_{1-}^{y-i-p} \times I, \end{aligned}$$

where for the integral in equation (C.4),

$$I = \frac{(-1)^{j+1} j!}{\{(Y_{\max}-y_0-i-k)(-\lambda) + [(k-l)+m+n+p]r_+ + [l+[y_0-(y-i)-m]+i-n+(y-i-p)]r_-\}^{j+1}} \tag{C.4'}$$

and for the moment generating function given by equation (C.7a),

$$I = \frac{-1}{s + \{(Y_{\max}-y_0-i-k)(-\lambda) + [(k-l)+m+n+p]r_+ + [l+[y_0-(y-i)-m]+i-n+(y-i-p)]r_-\}^{j+1}}. \tag{C.7a'}$$

First passage to $X = X_{\max} + 1$

Let Y_x denote a cell's value of Y when it first reaches the cell cycle state x. The probability Π that a cell has $Y_{X_{\max}+1}$ activated genes at the time of cell division is obtained by enumerating all the possible paths:

$$\begin{aligned} \Pi[(0, y_0) \to (X_{\max}+1, y_{X_{\max}+1})] = \sum_{y_1=0}^{Y_{\max}} \sum_{y_2=0}^{Y_{\max}} \cdots \sum_{y_{X_{\max}}=0}^{Y_{\max}} & \Pi[(0, y_0) \to (1, y_1)] \Pi[(1, y_1) \to (2, y_2)] \cdots \\ & \cdots \Pi[(X_{\max}-1, y_{X_{\max}-1}) \to (X_{\max}, y_{X_{\max}})] \Pi[(X_{\max}, y_{X_{\max}}) \to (X_{\max}+1, y_{X_{\max}+1})]. \end{aligned} \tag{C.8}$$

It is especially easy to perform this convolution if $X_{max}+1$ is some power of 2, since we may then factorize the matrix product:

$$\Pi[(0, y_0) \to (2^{m+1}, y_{2^{m+1}})] = \sum_{y_{2^m}=0}^{Y_{max}} \Pi[(0, y_0) \to (2^m, y_{2^m})] \cdot \Pi[(0, y_{2^m}) \to (2^m, y_{2^{m+1}})]. \quad \text{(C.9)}$$

Thus, equation (C.8) may be calculated recursively using equation (C.9), beginning with the use of equation (C.5)($j=0$). If $X_{max}+1$ is to a power of 2, then the above expression is still useful, since $X_{max}+1$ may be decomposed as the sum of powers of 2.

Now, consider a cell that undergoes the transition from $(X, Y)=(0, y_0)$ to $(X, Y)=(2, y_2)$. To calculate the moments for the time required to undergo this transition, it is useful to first calculate the cumulant (semi-invariant) moments from the moments about the origin, equation (C.6), since the cumulant for the sum of independent random variables equals the sum of the cumulants (of the same order) of the individual random variables that contribute to the sum [e.g. 169]. Let $C^{(j)}$ denote a cumulant of order j. Then, the first four cumulants are obtained from the moments given in equation (C.6), using the following formulae:

$$C^{(1)}[(0, y_0) \to (1, y_1)] = \langle A[(0, y_0) \to (1, y_1)] \rangle, \quad \text{(C.10a)}$$

$$C^{(2)}[(0, y_0) \to (1, y_1)] = \langle \{A[(0, y_0) \to (1, y_1)]\}^2 \rangle - \{C^{(1)}\}^2, \quad \text{(C.10b)}$$

$$C^{(3)}[(0, y_0) \to (1, y_1)] = \langle \{A[(0, y_0) \to (1, y_1)]\}^3 \rangle - 3C^{(1)}C^{(2)} - \{C^{(1)}\}^3 \quad \text{(C.10c)}$$

and

$$C^{(4)}[(0, y_0) \to (1, y_1)] = \langle \{A[(0, y_0) \to (1, y_1)]\}^4 \rangle - 6\{C^{(1)}\}^2 C^{(2)} - 4C^{(1)}C^{(3)} - \{C^{(1)}\}^4. \quad \text{(C.10d)}$$

The cumulants for the time required to make the transition from $X=0$ to $X=2$ are related to those for the transition from $X=0$ to $X=1$ by the expression

$$C^{(j)}[(0, y_0) \to (2, y_2)] = \sum_{y_1=0}^{Y_{max}} \Pi[(0, y_0) \to (1, y_1)] \cdot \{C^{(j)}[(0, y_0) \to (1, y_1)] + C^{(j)}[(0, y_1) \to (1, y_2)]\}. \quad \text{(C.11)}$$

Similarly, the cumulants for the time required to undergo the transition from $X=0$ to $X=2^{m+1}$ may be calculated from those for the transition from $X=0$ to $X=2^m$:

$$C^{(j)}[(0, y_0) \to (2^{m+1}, y_{2^{m+1}})] = \sum_{y_{2^m}=0}^{Y_{max}} \Pi[(0, y_0) \to (2^m, y_{2^m})] \cdot \{C^{(j)}[(0, y_0) \to (2^m, y_{2^m})] + C^{(j)}[(0, y_{2^m}) \to (2^m, y_{2^{m+1}})]\}. \quad \text{(C.12)}$$

APPENDIX D

Near "Steady State" Populations, Entropy of the Population and the Asymptotic Behavior of Cell Populations

For an arbitrary set of initial conditions, the time-course of the population described by equations (2a, b) will be a complicated sum of exponentials. As transients die out, the fractions $f(x, y; t)$ that are described by equations (6a–c) will be damped oscillations. This appendix explains how to calculate parameters that characterize the oscillations, using a standard procedure from the qualitative theory of differential equations [181]. The related topics of asymptotic stability and entropy will also be discussed here briefly, including the special cases of circadian rhythms and the kinetics of cell populations that are exposed periodically to cytotoxic agents.

Consider the case in which the distribution of cell cycle states (X) among the cells of the population is perturbed slightly from the "steady state", and in which the distribution of fibrillar centers (Y) is described by the "steady state" given in Appendix B. Then, the deviation from the "steady state" satisfies a simplified version of equations (14a,b):

$$\frac{d\Delta f(0, \cdot; t)}{d[\beta \langle Y \rangle t]} = -\frac{1}{\Omega}\Delta f(0, \cdot; t) + 2\Omega \Delta f(X_{max}, \cdot; t) - \Delta f(0, \cdot; t)\Delta f(X_{max}, \cdot; t) \quad \text{(D.1a)}$$

and

$$\frac{d\Delta f(x, \cdot; t)}{d[\beta \langle Y \rangle t]} = \Delta f(x-1, \cdot; t) - \frac{1}{\Omega}\Delta f(x, \cdot; t) - \Delta f(x, \cdot; t)\Delta f(X_{max}, \cdot; t) - 2(1-\Omega)\Omega^x \Delta f(X_{max}, \cdot; t). \quad \text{(D.1b)}$$

In the vicinity of the "steady state", the non-linear terms go as the square of the deviation and may be neglected. Then, equations (D.1a, b) become a set of linear differential equations with solutions of the form

$$\Delta f(x, \cdot; t) = \overline{\Delta f}(x) \exp(\beta \langle Y \rangle K t). \quad \text{(D.2)}$$

Substituting equation (D.2) into the linearized equations (D.1a, b), we obtain the eigenvalue equations:

$$2\Omega \overline{\Delta f}(X_{max}) - \left(K + \frac{1}{\Omega}\right)\overline{\Delta f}(0) = 0 \quad \text{(D.3a)}$$

and

$$\overline{\Delta f}(x-1) - \left(K + \frac{1}{\Omega}\right) - 2(1-\Omega)\Omega^x \overline{\Delta f}(X_{max}) = 0. \quad \text{(D.3b)}$$

Solving for $\overline{\Delta f}(0)$ in terms of itself, we obtain the characteristic polynomial equation

$$\left(K + \frac{1}{\Omega}\right)^{X_{max}} + 2(1-\Omega)\Omega \frac{1 - \left[\left(K + \frac{1}{\Omega}\right)\Omega\right]^{X_{max}}}{1 - \left[\left(K + \frac{1}{\Omega}\right)\Omega\right]} = \frac{2\Omega}{K + \frac{1}{\Omega}}. \quad \text{(D.4a)}$$

Let $r = K\Omega + 1$. Then, the simplified polynomial equation is

$$r^{X_{\max}+1} + (1-\Omega)\sum_{i=0}^{X_{\max}-1} r^{i+1} - \Omega = 0. \tag{D.4b}$$

Both the real and imaginary parts of the $X_{\max}+1$ roots of this equation are between -1 and 1. Therefore, all eigenvalues $K = (r-1)/\Omega$ have negative real parts. The one whose real part is least negative will dominate at large time, and its absolute value is a measure of the rate of damping of the $\Delta f(x, \cdot\,; t)$. Its imaginary part determines the frequency of the damped oscillations.

A "steady state", such as the one examined here, is said to be asymptotically stable if there exists a Lyapunov function for the system of equations. A Lyapunov function is a function that is always greater than or equal to zero, that equals zero when the system is in the "steady state" and whose time derivative is always less than or equal to zero. Clearly, if we multiply such a function by -1, the resulting function is always less than or equal to zero, and its time derivative is greater than or equal to zero. The latter convention is adopted in thermodynamics, in which the function is known as an entropy: the "steady state" corresponds to a state of maximum entropy. It is possible to construct an entropy when all of the eigenvalues of the linearized equation have negative real parts. To do so, we first need solutions to the (linearized) equation under the $X_{\max}+1$ initial conditions:

$$\Delta f(x, \cdot\,; 0) = 1 \quad \text{if} \quad x = i \quad (i = 0, 1, 2, \ldots, X_{\max}),$$
$$\Delta f(x, \cdot\,; 0) = 0 \quad \text{otherwise.} \tag{D.5}$$

Let $\Delta f(x, \cdot\,; t, i)$ denote the solution under the ith initial condition. If these particular solutions are known, the solution under arbitrary initial conditions is simply a superposition of the particular solutions. These particular solutions may be found by numerically integrating the linearized equations (D.1a, b) under the various initial conditions. They may also be found using the following linear transform method. Let $\tilde{\Delta} f(x, \cdot\,; s)$ denote the Laplace transform of the linearized equation (D.1), with initial conditions $\Delta f(x, \cdot\,; 0)$. Then, the transformed equations are

$$\left(s + \frac{1}{\Omega}\right)\tilde{\Delta} f(0, \cdot\,; s) = 2\Omega\tilde{\Delta} f(X_{\max}, \cdot\,; s) + \Delta f(0, \cdot\,; 0) \tag{D.6a}$$

and

$$\left(s + \frac{1}{\Omega}\right)\tilde{\Delta} f(x, \cdot\,; s) = \tilde{\Delta} f(x-1, \cdot\,; s) - [2(1-\Omega)\Omega^x]\tilde{\Delta} f(X_{\max}, \cdot\,; s) + \Delta f(x, \cdot\,; 0). \tag{D.6b}$$

Iterative substitution of one equation into the other leads to the solution

$$\tilde{\Delta} f(x, \cdot\,; s, i) = \frac{\left[\dfrac{2\Omega}{A^{x+1}} - \dfrac{2\Omega(1-\Omega)}{A^x}\cdot\dfrac{1-(\Omega A)^x}{1-\Omega A}\right]\dfrac{1}{A^{X_{\max}+1-i}}}{1 - \dfrac{2\Omega}{A^{X_{\max}+1}} + \dfrac{2\Omega(1-\Omega)}{A^{X_{\max}}}\cdot\dfrac{1-(\Omega A)^{X_{\max}}}{1-\Omega A}} + 1/[A^{x+1-i}] \quad \text{if} \quad (x+1-i) > 0,$$

where

$$A = [s/(\beta\langle Y\rangle)] + [1/\Omega]. \tag{D.7}$$

Inversion of the Laplace transform may then be performed numerically [227] to obtain the desired $\Delta f(x, \cdot\,; t, i)$. Once these fractions are known, we may construct the array

$$a(i,j) = \sum_{x=0}^{X_{\max}} \int_0^\infty \mathrm{d}t\, \Delta f(x, \cdot\,; t, i)\Delta f(x, \cdot\,; t, j). \tag{D.8}$$

Convergence of the integral is an immediate consequence of the fact that the eigenvalues have negative real parts.

Then, by Lyapunov's direct method, the following is an entropy, and the "steady state" is asymptotically stable:

$$S(\Delta f(0, \cdot\,; t), \Delta f(1, \cdot\,; t), \ldots, \Delta f(X_{\max}, \cdot\,; t)) = -\sum_{i=0}^{X_{\max}}\sum_{j=0}^{X_{\max}} a(i,j)\Delta f(i, \cdot\,; t)\Delta f(j, \cdot\,; t). \tag{D.9}$$

The entropy will increase in time, irrespective of the initial conditions, whether the system is initially close to the "steady state" or not. An example is provided in Fig. 13.

Not all cell cycle models exhibit the property of an asymptotically stable state of exponential growth. For example, models in which cell size increases exponentially cannot predict asymptotically stable growth if the rate of cell growth is an inherited property. Several recent articles have examined the conditions under which this type of model can be expected to show asymptotic stability [38, 39, 53, 228–232].

To complete the discussion of asymptotic stability, two related problems will now be outlined; circadian rhythms and the periodic killing of cells. Circadian rhythms are incorporated into cell cycle models by letting a model's parameters be periodic functions of time [175, 204, 205, 233–237]. Similarly, cytotoxicity is modelled by eliminating cells at periodic time intervals (see Section 8). In either case, asymptotic stability of the type mentioned above cannot exist since the fractions of cells in each of the cell cycle states will fluctuate periodically. However, for most linear models of either type, the number of cells as a function of time will have an asymptotic *envelope* that grows (or declines) exponentially. An example is provided in Fig. 18. The exponent characterizing the exponential growth (or decline) of the envelope, analogous to the Malthusian parameter, may be calculated by solving an eigenvalue equation to find the dominant eigenvalue (the spectral radius) that is predicted by the Perron–Frobenius theorem for irreducible non-negative matrices [238]. In the case of a differential equation with periodic coefficients (circadian rhythms), the analysis is known as Floquet theory [239]. The case of periodic cell killing is a generalization of Floquet theory [240]. Specifically, let $N(x, y;\ \tau,\ \{N(x, y; t=0)\})$ denote the number of cells in the (x, y) state at time τ, given that the number of cells in the various states at time zero was $\{N(x, y; t=0)\}$. Every τ minutes, cells are killed or converted to another state by our cytotoxic procedure. Let the number of cells after each episode of cytotoxicity be

$$N(x,y)\Big|_{\text{after}} = \sum_{x'=0}^{X_{\max}}\sum_{y'=0}^{Y_{\max}} \Phi(x, y; x', y')N(x', y')\Big|_{\text{before}}, \tag{D.10}$$

where $\Phi(x, y; x', y')$ represents the effect of the cytotoxic procedure. If

$$\sum_{x'=0}^{X_{max}} \sum_{y'=0}^{Y_{max}} \Phi(x, y; x', y') N(x', y'; \tau, \{N(x, y; 0)\}) = N(x, y; 0) \exp(k\tau), \tag{D.11}$$

then the number of cells in the population will be seen to increase (or decline) exponentially when examined at successive times, separated by the period τ. Floquet theory predicts that such a k exists (the spectral radius), that such an $\{N(x, y; t = 0)\}$ exists (the corresponding eigenvector) and that the population will evolve asymptotically towards this state of growth, irrespective of its initial condition. In general, calculation of the k and $\{N(x, y; t = 0)\}$ will be most easily performed by numerically integrating the equations describing the population's dynamics. Note that the population will oscillate asymptotically at the driving period τ for much the same reason that a linear, damped, driven electronic oscillator follows its driving force. In fact, many conventional engineering concepts may be applicable to the linear cell kinetic model (Q of the system, parametric amplification etc) as a consequence of the linearity of the population dynamics. A test for the absence of linearity is to drive the population at a pair of frequencies to see whether the asymptotic oscillations occur not only at the driving frequencies, but also at harmonic and sideband frequencies.